

Quality-diversity in Dissimilarity Spaces

Steve Huntsman
steve.huntsman@str.us

ABSTRACT

The theory of magnitude provides a mathematical framework for quantifying and maximizing diversity. We apply this framework to formulate quality-diversity algorithms in generic dissimilarity spaces. In particular, we instantiate a very general version of Go-Explore with promising performance for challenging and computationally expensive objectives, such as arise in simulations. Finally, we prove a result on diversity at scale zero that is interesting in its own right and consider its implications for our algorithm.

CCS CONCEPTS

• **Theory of computation** → **Mixed discrete-continuous optimization**.

KEYWORDS

Quality-diversity optimization, dissimilarity, magnitude

1 INTRODUCTION

The survival of a species under selection pressure is a manifestly challenging optimization problem, jointly solved by evolution many times over despite omnipresent maladaptation [17]. This suggests that many objective functions that are hard to optimize (and frequently, also hard to evaluate) may admit a diverse set of inputs that perform well even if they are not local extrema. *Quality-diversity* (QD) algorithms [24, 100] such as NSLC [71], MAP-Elites [87], and their offshoots, seek to produce such sets of inputs, typically by discretizing the input space into “cells” and returning the best input found for each cell. QD differs from multimodal optimization by exploring regions of input space that need not have extrema.¹

The link between exploration and diversity in ecosystems is that “nature abhors a vacuum in the animate world” [49]. A similar link informs optimization algorithms [53–55]. The key construction is a mathematically principled notion of diversity that generalizes information theory by incorporating geometry [72, 73]. It singles out the Solow-Polasky diversity [111] or *magnitude* of a finite space endowed with a symmetric dissimilarity in relation to the “correct” definition (1) of diversity that uniquely satisfies various natural desiderata. The uniqueness of a diversity-maximizing probability distribution has been established [74], though to our knowledge the only applications to optimization are presently [53–55].

In this paper, which elaborates on the conference paper [56], we apply the notion (1) of diversity to QD algorithms for the first time by producing a formalization of the breakthrough Go-Explore framework [33] suited for computationally expensive objectives in very general settings. The algorithm requires very little tuning and its only requirements are

¹Another practical (if not theoretical) difference between QD and multimodal optimization algorithms is that the former are often explicitly intended to operate in a (possibly latent) low-dimensional behavioral or phenotypical space, but this is mostly irrelevant from the primarily algorithmic point of view we concern ourselves with here. The key algorithmic point is to consider a “pullback” dissimilarity: for this, see the archetypal class of objectives discussed in §3.

- a symmetric, nondegenerate dissimilarity (not necessarily satisfying the triangle inequality) that is efficient to evaluate;
- a mechanism for globally generating points in the input space (which need not span the entire space, since we can use the output of one run of the algorithm to initialize another);
- an efficient mechanism for locally perturbing existing points;
- and a mechanism for estimating the objective that permits efficient evaluation: e.g., interpolation using polyharmonic radial basis functions [19] or a neural network.

Other than these, the algorithm’s only other inputs are a handful of integer parameters that govern the discretization of the input space and the effort devoted to evaluating the objective and its cheaper estimate. Our examples repeatedly reuse many values for these.

The paper is organized as follows. In §2, we introduce the concepts of magnitude and diversity. In §3, we outline the Go-Explore framework in the context of dissimilarity spaces. In §4 we construct a probability distribution for “going” that balances exploration and exploitation. We discuss local exploration mechanisms in §5. In §6 we provide a diverse set of examples. Finally, in §7 we analyze the effects of considering an extremal notion of diversity before concluding in §8.

2 MAGNITUDE AND DIVERSITY

For details on the ideas in this section, see §6 of [72]; see also [54] for a slightly more elaborate retelling.

The notion of magnitude that we will introduce below has been used by ecologists to *quantify* diversity since the work of Solow and Polasky [111], but much more recent mathematical developments have clarified the role that magnitude and the underlying concept of weightings play in *maximizing* a more general and axiomatically supported notion of diversity [72, 74]. We will describe these concepts in reverse order, moving from diversity to weightings and magnitude in turn before elaborating on them.

A square nonnegative matrix Z is a *similarity matrix* if its diagonal is strictly positive. Now the *diversity of order q* for a probability distribution p and similarity matrix Z on the same space is

$$D_q^Z(p) := \exp\left(\frac{1}{1-q} \log \sum_{j:p_j>0} p_j (Zp)_j^{q-1}\right) \quad (1)$$

for $1 < q < \infty$, and via limits for $q = 1, \infty$.² This is the “correct” measure of diversity in essentially the same way that Shannon entropy is the “correct” measure of information.

If the similarity matrix Z is symmetric, then it turns out that the diversity-maximizing distribution $\arg \max_p D_q^Z(p)$ is actually independent of q . There is an algorithm to compute this distribution that we will discuss below, and in practice we can usually perform a nonlinear scaling of Z to ensure the distribution is efficiently

²The logarithm of (1) is a “similarity-sensitive” generalization of the Rényi entropy of order q . For $Z = I$, the Rényi entropy is recovered, with Shannon entropy for $q = 1$.

computable. We restrict attention to similarity matrices of the form

$$Z = \exp[-td] \quad (2)$$

where $(\exp[M])_{jk} := \exp(M_{jk})$, $t \in (0, \infty)$ is a scale parameter, and d is a square symmetric *dissimilarity matrix*: i.e., its entries are in $[0, \infty]$, with zeros on and only on the diagonal.³

A *weighting* w is a vector satisfying

$$Zw = 1, \quad (3)$$

where the vector of all ones is indicated on the right. A *coweighting* is the transpose of a weighting for Z^T . If Z has both a weighting w and a coweighting, then its *magnitude* is $\sum_j w_j$, which also equals the sum of the coweighting components. In particular, if Z is invertible then its magnitude is $\sum_{jk} (Z^{-1})_{jk}$. The theory of weightings and magnitude provide a very attractive and general notion of size that encodes rich scale-dependent geometrical data [75].

Example 1. Take $\{x_j\}_{j=1}^3$ with $d_{jk} := d(x_j, x_k)$ given by $d_{12} = d_{13} = 1 = d_{21} = d_{31}$ and $d_{23} = \delta = d_{32}$ with $\delta < 2$. A straightforward calculation of (3) using (2) is shown in Figure 1 for $\delta = 10^{-3}$. At $t = 10^{-2}$, the “effective size” of the nearby points is ≈ 0.25 , and that of the distal point is ≈ 0.5 , so at this scale the “effective number of points” is ≈ 1 . At $t = 10$, the effective number of points is ≈ 2 . Finally, at $t = 10^4$, the effective number of points is ≈ 3 .

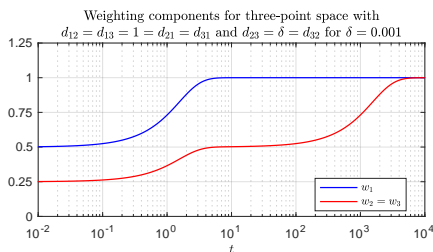


Figure 1: The magnitude $w_1 + w_2 + w_3$ of an isocoles dissimilarity space is a scale-dependent “effective number of points.”

For a symmetric similarity matrix Z , the positive weighting of the submatrix on common row and column indices that has the largest magnitude is unique and proportional to the diversity-saturating distribution for *all* values of the free parameter q in (1), and this magnitude equals the maximum diversity. Because of the exponential number of subsets involved, in general the diversity-maximizing distribution is NP-hard to compute, though cases of size ≤ 25 are easily handled on a laptop.

The algorithmic situation improves radically if besides being symmetric, Z is also positive definite⁴ and admits a positive weighting w (which is unique by positive-definiteness). Then

$$\arg \max_p D_q^Z(p) = \frac{w}{1^T w}, \quad (4)$$

³Henceforth we assume symmetry and nondegeneracy for d unless stated otherwise. We will also write d for a symmetric, nondegenerate *dissimilarity* $d : X^2 \rightarrow [0, \infty]$ with $d(x, x) \equiv 0$ and $x \neq x' \Rightarrow d(x, x') \neq 0$. Here X is called a *dissimilarity space*. Note that d (as a matrix or function) is *not* assumed to satisfy the triangle inequality.

⁴If d is the distance matrix corresponding to (e.g.) a finite subset of Euclidean space, $Z = \exp[-td]$ is automatically positive definite: see Theorem 3.6 of [82].

i.e., this weighting is proportional to the diversity-maximizing distribution, and linear algebra suffices to obtain it efficiently.⁵

To engineer this situation, we take $Z = \exp[t_+ d]$, where the *strong cutoff* t_+ is the minimal value such that $\exp[-td]$ is positive semidefinite and admits a nonnegative weighting for any $t > t_+$. This is guaranteed to exist and can be computed using the bounds

$$\frac{\log(n-1)}{\min_j \max_k d_{jk}} \leq t_d \leq \frac{\log(n-1)}{\min_j \min_{k \neq j} d_{jk}} \quad (5)$$

where t_d is the minimal value such that $\exp[-td]$ is diagonally dominant (i.e., $1 > \max_j \sum_{k \neq j} \exp(-td_{jk})$) and hence also positive definite for any $t > t_d$ [54].

3 GO-EXPLORE

The animating principle of Go-Explore is to “first return, then explore” [33]. This is a simple but powerful principle: by returning to previously visited states, Go-Explore avoids two pitfalls common to most sparse reinforcement learning algorithms such as [50]. It does not prematurely avoid promising regions, nor does it avoid underexplored regions that have already been visited.

The basic scheme of Go-Explore is to repeatedly

- probabilistically sample and **go** to an elite state;
- **explore** starting from the sampled elite;
- map resulting states to a cellular discretization of space;
- update the elites in populated cells.

This scheme has achieved breakthrough performance on outstanding challenge problems in reinforcement learning. Viewing it in the context of QD algorithms, we produce in Algorithm 1 a specific formal instantiation of Go-Explore for computationally expensive objectives on dissimilarity spaces while illustrating ideas and techniques that apply to more general settings and instantiations.

The basic setting of interest to us is a space X endowed with a nondegenerate and symmetric (but not necessarily metric) dissimilarity $d : X^2 \rightarrow [0, \infty]$ and an objective $f : X \rightarrow \mathbb{R}$ for which we want a large number of diverse inputs x (in the sense of (1)) that each produce relatively small values of f . We generally assume that f is expensive to compute, so we want to evaluate it sparingly.

Although we assume the existence of a “global generator” that produces points in X , it does not need to explore X globally: running our algorithm multiple times in succession (with elites from one run serving as “landmarks” in the next) addresses this. Similarly, although we assume the existence of a “local generator” in the form of a probability distribution, we do not need to know much about it—only that it be parametrized by a current base point $x \in X$ and some scalar parameter θ , and that we can efficiently sample from it.

A global generator suffices to provide a good discretization of a dissimilarity space along the lines of Algorithms 2 and 3, generalizing the approach of [118]. Magnitude satisfies an asymptotic (i.e., in the limit $t \uparrow \infty$) inclusion-exclusion formula for compact convex bodies in Euclidean space [45], and more generally appears to be approximately submodular.⁶ This suggests using the standard greedy

⁵In Euclidean space, the geometrical manifestation of diversity maximization via weightings is an excellent scale-dependent boundary/outlier detection mechanism [20, 54, 121]. A technical explanation for this boundary-detecting behavior draws on the potential-theoretical notion of Bessel capacities [83].

⁶ $F : 2^\Omega \rightarrow \mathbb{R}$ is submodular iff $\forall X \subseteq \Omega$ and $x_1, x_2 \in \Omega \setminus X$ s.t. $x_1 \neq x_2$, $F(X \cup \{x_1\}) + F(X \cup \{x_2\}) \geq F(X \cup \{x_1, x_2\}) + F(X)$. Let $\Omega = \{(1, 0), (0, 1), (-1, 0), (2, 0)\}$

approach for approximate submodular maximization [69, 88] despite the fact that we do not have any theoretical guarantees. In practice this works well: by greedily maximizing the magnitude of a fixed-size subset of states, Algorithm 2 produces a set of diverse landmarks, as Figure 3 shows. Ranking the dissimilarities of these landmarks to a query point yields a good locality-sensitive hash [4, 25, 46, 58, 64, 76, 90, 110, 114].⁷ See Figure 3.

Although we generally assume an ability to produce a computationally cheap surrogate for f and the availability of parallel resources for evaluating f in much the same manner as [42, 66, 124], most of our approach can be adapted to cases where either of these assumptions do not hold: see §E of the supplement.

An archetypal class of example objectives is of the form $f = \phi \circ \gamma$, where $\gamma : X \rightarrow Y$ and $\phi : Y \rightarrow \mathbb{R}$ respectively embody a computationally expensive “genotype to phenotype” simulation and a fitness function such as $\phi(y) = \min_{\omega \in \Omega} d_Y(y, \omega)$ for some finite $\Omega \subset Y$ (e.g., representing desired outcomes of different tasks) and with $d(x, x') := d_Y(\gamma(x), \gamma(x'))$ a pullback distance.

This degree of generality is useful. In applications X and/or Y might be a pseudomanifold or a discrete structure like a graph or space of variable-length sequences, so that d is not (effectively anything like) Euclidean. Indeed, a now-classical result (phenomenologically familiar to users of multidimensional scaling) is that finite metrics (to say nothing of more general dissimilarities *per se*) are generally not even embeddable in Euclidean space [15, 78].

A class of problems where Y is a graph arises in automatic scenario generation [7, 39, 77, 80, 89] where simulations involve a flow graph or finite automaton of some sort, e.g. testing and controlling machine learning, cyber-physical, and/or robotic systems.⁸

Another attractive class of potential applications, in which X is a space of variable-length sequences, is the design of diverse proteins and/or chemicals in high-throughput virtual screening [48]. In pharmacological settings, a quantitative structure–activity relationship is an archetypal objective [105]. For example, consider the problem of protein design in the context of an mRNA vaccine [95] where diversity could aid in the development of universal vaccines that protect against a diverse set of viral strains [47, 67, 86, 97]. Proteins are conveniently represented using nucleic/amino acid sequences, and sequence alignment and related techniques give relevant dissimilarities [57, 103]. Using AlphaFold [63, 117] for protein structures and complementary deep learning techniques such as [81], it is possible to estimate molecular docking results in about 30 seconds. Meanwhile, more accurate and precise results from absolute binding free energy calculations require about a day with a single GPU [29].⁹ Our approach appears to offer favorable use of parallel resources in realistic applications of this sort [61].

In still other applications, Y might be a latent space of the sort produced by an autoencoder or generative adversarial network [38, 43]. Such applications are not as directly targeted by our instantiated

algorithm since in practice such spaces are treatable as locally Euclidean (though only as pseudomanifolds *versus* manifolds *per se* due to singularities) and more specialized instantiations might be suitable. By the same token, we basically ignore the “behavioral” focus of many QD algorithms: in our intended applications, the local (and frequently global) generators already operate on reasonably low-dimensional feature (or latent) spaces, or the dissimilarity is pulled back from such a space. That said, engineering landmarks rather than using Algorithm 2 can produce cells that follow a grid pattern and/or enable internal behavioral representations.

Algorithm 1 GOEXPLOREDISSIMILARITY($f, d, L, T, K, G, M, g, \mu$)

Require: Objective $f : X \rightarrow \mathbb{R}$, dissimilarity $d : X^2 \rightarrow [0, \infty]$, number of landmarks L , number of initial states $T \geq L$, rank cutoff $K \ll L$, global generator $G : \mathbb{N} \rightarrow X$, evaluation budget M , local generator probability distributions $g(x'|x, \theta)$, and maximum “per-expedition” exploration effort μ

```

1: Generate landmarks  $\subset$  initial states  $X'$  using  $G$  // Algorithm 2
2: Evaluate  $f$  on  $X'$ 
3: Evaluate  $\sigma^{(K)}$  on  $X'$  and initialize history  $h$  // Algorithm 3
4: while  $|h| < M$  do
5:    $E \leftarrow \bigcup_{\tau} \{\arg \min_{x \in h: \sigma^{(K)}(x) = \tau} f(x)\}$  // Elites
6:   Compute weighting  $w$  at scale  $t_+$  on  $E$ 
7:   Form  $p \propto \exp([\log w]_{\wedge} - [f]_E)_{\wedge}$  // §4
8:   Compute best feasible lower bound  $b \leq \mathbb{E}_p(C_{\lceil |E|/2 \rceil})$  // §C
9:   for  $b$  steps do
10:    Sample  $x \sim p$ 
11:    Compute exploration effort  $\mu_* \in [\mu]$  // §5.1
12:     $U \leftarrow$  set of the  $\min\{|h|, \lceil \mu/2 \rceil\}$  states in  $h$  nearest to  $x$ 
13:     $V \leftarrow \{y \in h : \sigma^{(K)}(y) = \sigma^{(K)}(x)\}$ 
14:    Form local estimate  $\hat{f}$  of  $f$  using data on  $U \cup V$  // §5.2
15:     $\theta \leftarrow \max_{y \in E} d(x, y)$  // §5.3
16:    Sample  $(x'_j)_{j=1}^{2\mu} \sim g^{\times 2\mu}(\cdot|x, \theta)$ 
17:    while  $|\{x'_j : \sigma^{(K)}(x'_j) = \sigma^{(K)}(x)\}| < 2\mu/4$  do
18:       $\theta \leftarrow \theta/2$ ; sample  $(x'_j)_{j=1}^{2\mu} \sim g^{\times 2\mu}(\cdot|x, \theta)$ 
19:    end while
20:    Get weighting  $w'$  at scale  $t'_+$  on  $\Lambda := \{x'_j\}_{j=1}^{2\mu} \cup U \cup V$ 
21:    Normalize  $\hat{f}|_{\Lambda}$  and  $-w'$  to zero mean and unit variance
22:    Compute Pareto domination of  $(\hat{f}|_{\Lambda}, -w')$  // §5.4
23:     $X' \leftarrow \min\{\mu_*, M - |h|\}$  least dominated pairs
24:  end for
25:  Evaluate  $f$  and  $\sigma^{(K)}$  on  $X'$ ; update  $h$ 
26: end while

```

Ensure: h (and E of globally diverse/locally optimal elites as above)

4 GOING

A distribution over cells drives the “go” process. We balance exploration of the space X and exploitation of the objective f , respectively via a diversity-saturating probability distribution (4) and a distribution proportional to $\exp(-\beta f)$. Rather than taking β as a variable regularizer, we use it to remove a degree of freedom. Define

$$[\phi]_{\wedge} := \frac{\phi - \text{median } \phi}{\max \phi - \text{median } \phi} \quad (6)$$

endowed with Euclidean distance; let $X = \{(1, 0), (0, 1)\}$; let $x_1 = (-1, 0)$, and $x_2 = (2, 0)$. Then (using an obvious notation) $\text{Mag}(X \cup \{x_1\}) + \text{Mag}(X \cup \{x_2\}) \approx 4.1773$ while $\text{Mag}(X \cup \{x_1, x_2\}) + \text{Mag}(X) \approx 4.1815$, so magnitude is not submodular.

⁷A dissimilarity on the symmetric group S_n can be used to query: see §B.1 (supplement).

⁸This is related to fuzzing [13, 79, 123, 126], but with an emphasis on phenomenology rather than finding bugs, and a different computational complexity regime.

⁹For chemical drug design, a convenient representation is the SMILES language [120], and relevant dissimilarities include [91, 107]. Here, a chemical drug–target interaction objective can be estimated using deep learning approaches such as [44, 65, 109].

Algorithm 2 GENERATEDIVERSELANDMARKS(d, L, T, G)

Require: Dissimilarity $d : X^2 \rightarrow [0, \infty]$, number of landmarks L , number of state generations $T \geq L$, global state generator $G : \mathbb{N} \rightarrow X$ that is one-to-one on $[T]$

```

1: for  $i$  from 1 to  $L$  do
2:    $x_i \leftarrow G(i)$  // State
3:    $I(i) \leftarrow i$  // Landmark index
4: end for
5:  $D \leftarrow d_{\{x_{I(i)}, i \in [L]\}}$  // Dissimilarity matrix
6:  $t \leftarrow t_+(D)$  // Strong cutoff
7:  $w \leftarrow \exp[-tD] \setminus 1$  // Weighting
8:  $M \leftarrow 1^T w$  // Magnitude
9: for  $i$  from  $L+1$  to  $T$  do
10:   $i' \leftarrow \arg \min w$  // State with least weighting component
11:   $x_i \leftarrow G(i)$  // Candidate state
12:   $I' \leftarrow I$  // Candidate landmark indices
13:   $I'(i') \leftarrow i$  // Try current index for landmark
14:   $D' \leftarrow d_{\{x_{I'(i)}, i \in [L]\}}$  // Candidate dissimilarity matrix
15:   $w' \leftarrow \exp[-tD'] \setminus 1$  // Candidate weighting
16:   $M' \leftarrow 1^T w'$  // Candidate magnitude
17:  if  $M' > M$  then
18:     $I \leftarrow I', M \leftarrow M'$  // Accept candidate
19:  end if
20: end for

```

Ensure: Initial states $\{x_i\}_{i=1}^T$, L landmark indices in $I \subseteq [T]$

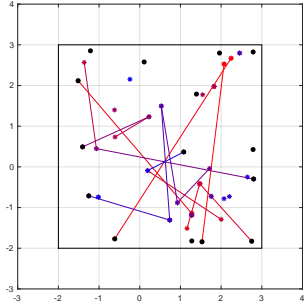


Figure 2: Algorithm 2 generates $L = 15$ landmarks shown as black dots (\bullet) among $T = \lceil L \log L \rceil = 41$ states with $G =$ sampling from $\mathcal{U}([-2, 3]^2)$. Non-landmark states are shown as asterisks ($*$) colored from red to blue in order of generation. Replacements of prior landmarks are indicated with lines in the same color scheme. At the end, landmarks are dispersed.

Algorithm 3 STATECELL($d, \{x_i\}_{i=1}^T, I, K, x$)

Require: Dissimilarity $d : X^2 \rightarrow [0, \infty]$, states $\{x_i\}_{i=1}^T$, landmark indices I with $L := |I| \leq T$, rank cutoff $K \leq L$, state $x \in X$

```

1: Sort to get  $\sigma$  such that  $d(x, x_{I(\sigma(1))}) \leq \dots \leq d(x, x_{I(\sigma(L))})$ 
2:  $\sigma^{(K)}(x) \leftarrow (\sigma(1), \dots, \sigma(K))$  //  $K$  closest landmarks (sorted)

```

Ensure: Cell identifier $\sigma^{(K)}(x)$

and the “go distribution”

$$p \propto \exp([\log w]_{\wedge} - [f|_E]_{\wedge}), \quad (7)$$

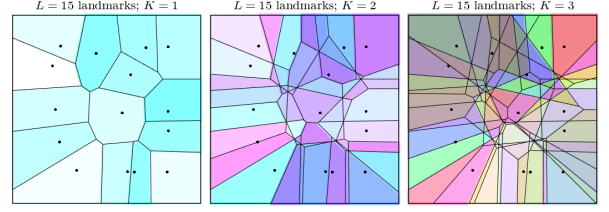


Figure 3: (All axes are $[-3, 4]^2$.) Algorithm 3 maps states to cells. $L = 15$ landmarks are shown as black dots (\bullet); these are iteratively selected from $T = \lceil L \log L \rceil = 41$ states with $G =$ sampling from $\mathcal{U}([-2, 3]^2)$ as described in Algorithm 2. Landmarks are mostly dispersed near the boundary of the sampling region. (Left; [resp., center; right]) Cells with $K = 1$ (resp., $K = 2; 3$) are all intersections of Voronoi cells of landmarks with 0 (resp., 1; 2) landmarks omitted. Many of the L^K notional cells are degenerate.

where the weighting w is computed for the set E of elites at scale t_+ .¹⁰ The distribution p encourages visits to cells whose elites contribute to diversity and/or have the lowest objective values. As elites improve, p changes over time, reinforcing the “go” process.

We want to sample from p to go to enough elites for exploration, but not so often as to be impractical. Meanwhile, to mitigate bias, we sample over the course of discrete epochs. As §C of the supplement details and Algorithm 1 requires, we efficiently compute a good lower bound on the expected time for the event C_m of visiting m of n elites via IID draws from the distribution $p \equiv (p_1, \dots, p_n)$. This lower bound is the number of iterations in the inner loop of Algorithm 1.

5 EXPLORING

In general, the entire exploration mechanism in Algorithm 1 should be tailored to the problem under consideration. Nevertheless, for the sake of striking a balance between specificity and generality we outline elements of an exploration mechanism that works “out of the box” on a variety of problems, as demonstrated in §6.

5.1 Exploration Effort

If the last two visits to a cell have (resp., have not) improved its elite, we spend more (resp., less) effort exploring on the next visit. Let f_- denote the elite objective from the penultimate visit, and f_0 the elite objective from the last visit. Let μ_- and μ_0 be the corresponding efforts (i.e., number of exploration steps). If we assume f is (empirically) normalized to take values in the unit interval, then $-1 \leq -(f_0 - f_-) \leq 1$. At the lower end, $f_0 - f_- = 1$, which is the worst; at the upper end, $f_0 - f_- = -1$, which is the best. We therefore assign exploration effort

$$\mu_+ = \lceil \min\{\max\{1, 2^{-(f_0 - f_-)} \mu_0\}, \mu\} \rceil, \quad (8)$$

where $\mu \in \mathbb{N}$ is the maximum exploration effort per “expedition.”

¹⁰The weighting w at scale t_+ (and (4)) has one entry equal to zero by construction. Therefore the corresponding entry of $\log w$ is $-\infty$ and we cannot get finite minima or moments, which motivates the normalization (6).

If and when μ_+ is unity for long enough across cells, it makes sense to halt Algorithm 1 before reaching M function evaluations: however, we do not presently do this.

5.2 Estimating the Objective Function

It is generally quite useful to leverage an estimate or *surrogate* \hat{f} to optimize an objective f whose evaluation is computationally expensive. It is possible to estimate objectives in very general contexts: e.g., for X a (di)graph endowed with a symmetric dissimilarity d , via graph learning and/or signal processing techniques [122].

In the more pedestrian and common settings $X \in \{\mathbb{R}^n, \mathbb{Z}^n, \mathbb{F}_2^n\}$, a straightforward approach to estimation is furnished by radial basis function interpolation [19] using linear (or more generally, polyharmonic) basis functions that require no parameters. Our code is built with this particular approach in mind.

5.3 Bandwidth for Random Candidates

The scalar *bandwidth* parameter θ in the “local generator” $g(x'|x, \theta)$ corresponds to, e.g., the standard deviation in a spherical Gaussian for $X \in \{\mathbb{R}^N, \mathbb{Z}^N\}$,¹¹ or the parameter in a Bernoulli trial. The idea is that θ governs the locality properties of g , with θ large (resp., small) approximating a uniform (resp., point) distribution on X . Note that if we have *any* mechanism for locally perturbing x , then repeating this θ times allows us to introduce a notion of bandwidth.

Now we want to be able to set θ so that we actually do explore, but only locally (for otherwise we might as well just evaluate f on points produced by G), i.e., we want to explore within and possibly just next to a cell. There is a simple way to do this provided that everything except evaluating f is fast and efficient (which we assume throughout). The idea is to sample from $g(\cdot|x, \theta)$ with a default (large) value for θ to generate a large number of “probes” widely distributed in X . We then decrease θ and sample again until a significant plurality of probes are in the same cell as the elite x .

Initially, we set $\theta = \max_{y \in E} d(x, y)$. Although this makes sense for g a Gaussian and still generally works for bit flips (albeit at the minor cost of probing until $\theta < 1$), some care should be exercised to ensure the definition of g and the initialization of θ are both compatible with the problem instance at hand.

5.3.1 Generator Adaptation. An alternative approach is to estimate the optimal parameter (here not necessarily scalar) of a local generator g . It should often be possible to borrow from CMA-ES [51] by taking the best performing probes and using them to update the covariance of (e.g.) a Gaussian. We forego this here in the interest of generality, though it is likely to be very effective [40].

5.4 Pareto Dominance

We assume that we can evaluate f in parallel and produce an estimate/surrogate \hat{f} that is inexpensive to evaluate. It is advantageous to evaluate f at points where we expect it to be more optimal based on \hat{f} , as well as at points that increase potential diversity (i.e., a weighting component) relative to prior evaluation points.

¹¹Perhaps surprisingly, sampling from the discrete Gaussian on $X = \mathbb{Z}^N$ is very hard [2]. Even producing a discrete Gaussian with specified moments is highly nontrivial [3]. For these reasons we prefer the simple expedient of rounding (away from zero) samples from a continuous Gaussian.

Given competing objectives α_i on a set Λ , we say the *Pareto domination* of $\lambda \in \Lambda$ is $\max_{\lambda' \in \Lambda} \min_i [\alpha_i(\lambda) - \alpha_i(\lambda')]$. In our algorithm, we take Λ to be the union of the set of probes with a set U of nearby states in the evaluation history and the set V of states in the evaluation history that belong to the same cell as the current elite x . We take $\alpha_1 = [\hat{f}]_{\parallel}$ and $\alpha_2 = [-w']_{\parallel}$, where w' is the weighting on Λ at scale t_+ and $[\cdot]_{\parallel}$ indicates a normalization to zero mean and unit variance. The points that are least Pareto dominated form a reasonable trade space between exploration and evaluation.

6 EXAMPLES

6.1 $X = \mathbb{R}^N$

We consider the Rastrigin function (see left panel of Figure 4)

$$f(x) = A \cdot N + \sum_{j=1}^N (x_j^2 - A \cos(2\pi x_j)) \quad (9)$$

on \mathbb{R}^N with the usual choice $A = 10$. This has a single global minimum at the origin and local minima on \mathbb{Z}^N . It (or a variant thereof) is commonly used as a test objective for QD [22, 30] as well as global optimization problems. Figure 4 (right) and Figure 5 show the output of Algorithm 1 for varying evaluation budgets.

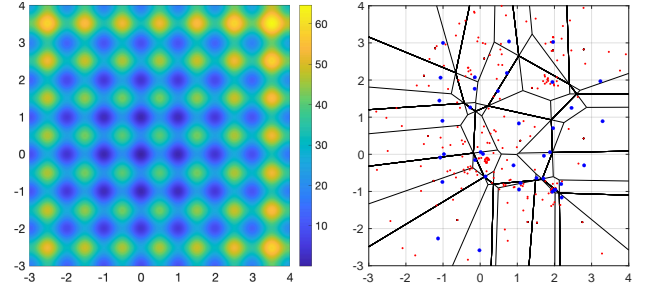


Figure 4: (Left) Plot of (9) on $[-3, 4]^2$. (Right) Output of Algorithm 1 for $M = 300$ evaluations of (9) for $N = 2$ with $L = 15$, $T = \lceil L \log L \rceil = 41$, and $K = 2$. To break symmetry, $G = \text{sampling from } \mathcal{U}([-2, 3]^N)$. Landmarks/cells are as in Figure 3. $g(\cdot|x, \theta) = \text{sampling from } \mathcal{N}(x, \theta^2 I)$; maximum per-expedition exploration effort $\mu = 128$. Evaluated points are shown as small red dots (•); elites as larger blue dots (•).

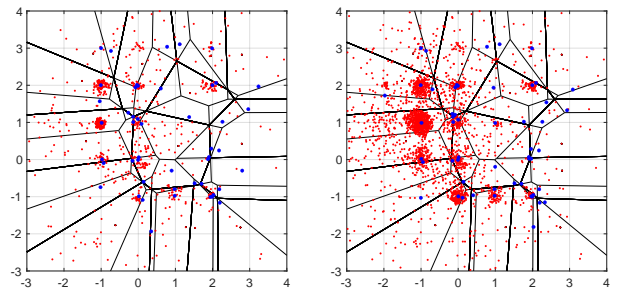


Figure 5: (Left) As in the right panel of Figure 4, but for $M = 1000$. The elite near $(1, 1)$ moved near $(1, 0)$. (Right) $M = 3000$.

6.1.1 *Benchmarking.* Because the cells produced by Algorithm 2 are irregular, it is difficult to compare our approach to most QD algorithms, especially using a QD score [100], which is the special case $WQD(1, f)$ of

$$WQD(w, \hat{f}) := |\text{supp } w| \cdot \frac{w^T \hat{f}}{w^T \mathbf{1}}, \quad (10)$$

where w is typically a solution of (3).¹² There are two possible workarounds: substitute regular cells, or consider a more “light-weight” version of the same approach. While the former option is superficially attractive in that we can compare to a notional reference algorithm, in practice there are only reference implementations of otherwise partially specified algorithms. Aligning a reference algorithm with Algorithm 2 would force us to consider low-dimensional problems that are comparatively disadvantageous as discussed shortly below. Since we already know Go-Explore is a high-performing class of algorithms, the latter option therefore is more informative (and though it does not preclude the former, we restrict consideration to it here).

Specifically, we consider a “baseline” version of Go-Explore with several specific and simple choices as described in §F of the supplement: note in particular that the chosen covariances for g therein are fairly well matched to the geometry of the problem.¹³ The results of this and Algorithm 1 with the same settings as in §6.1 are shown in Figure 6. There is a significant advantage for Algorithm 1 in dimensions $N \in \{10, 30\}$. For dimensions 3 and 100, the advantage lessens (not shown). In the former case, this is due to the low dimensionality that outweighs any marginal gains due to more precise exploitation of local minima. In the latter case, the problem becomes sufficiently difficult and the evaluation budget low enough that the advantages of Algorithm 1 cannot yet manifest.

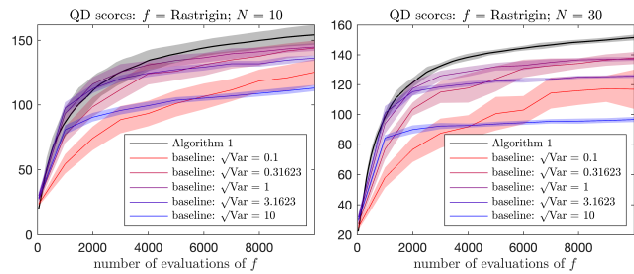


Figure 6: QD scores for Algorithm 1 and a “baseline” Go-Explore variant for varying bandwidths applied to the objective (9) (normalized to be in $[0, 1]$) in dimensions (left) $N = 10$ and (right) $N = 30$. Results are averaged with standard deviations indicated. (We elected not to normalize by the nominal number of possible cells.)

6.2 $X = \mathbb{Z}^N$

Only minor changes are required to demonstrate Algorithm 1 on a nontrivial problem on a discrete lattice. Here we take a scale

¹²The usual QD score $WQD(1, f)$ typically approximates (10) well in practice.

¹³The bandwidth for which the resulting Gaussian most nearly approximates the objective at the origin (up to an affine transformation) is approximately 0.2.

parameter $\lambda \in \mathbb{Z}_+$ and consider (9) on \mathbb{Z}^2 under the substitution $x \leftarrow x/\lambda$, while also scaling the domain in the same way. This has minima at $(\lambda\mathbb{Z})^2$, with the global minimum at the origin as before. By using the same pseudorandom number generator seed (which we normally do anyway for reproducibility), we can see a very similar variant of §6.1 emerge: see §G of the supplement.

6.3 $X = \mathbb{F}_2^N$

For binary problems, we embed \mathbb{F}_2 in \mathbb{Z} via $0 \mapsto 0$ and $1 \mapsto 1$.

The Sherrington-Kirkpatrick (SK) spin glass objective is [14, 93]

$$f(s) = \frac{1}{\sqrt{N}} \sum_{jk} J_{jk} s_j s_k, \quad (11)$$

where $s \in \{\pm 1\}^N$ is a spin configuration and J is a symmetric $N \times N$ matrix with IID $\mathcal{N}(0, 1)$ entries. It is a classic result that optimizing (11) is NP-hard, although there is an $O(N^2)$ algorithm that approximates the optimum with high probability [84].¹⁴ The underlying phenomenology is that (SK and more general) spin glasses have barrier trees¹⁵ that exhibit fractal and hierarchical characteristics [41, 125]. These same adjectives describe the landscape of (11), explaining why a near-optimum can be rapidly identified (i.e., via a coarse approximation of the landscape) yet an exact optimum still requires exponential time to identify in general. Figure 7 shows the performance of Algorithm 1 on an instance of (11) with $N = 20$.

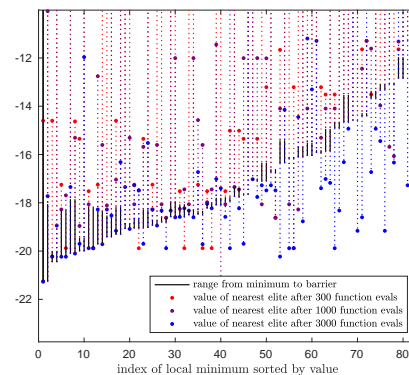


Figure 7: Performance of Algorithm 1 on (11) with $N = 20$, $d(s, s') := d_H^{1/2}(b, b')$ for $d_H = \text{Hamming distance}$ and $b := (s + 1)/2$, $L = 10$, $T = \lceil L \log L \rceil = 24$, $K = 2$, $G = \text{sampling from } \mathcal{U}(\mathbb{F}_2^N)$, g a Bernoulli bit flipper, and $\mu = 128$. There are $2^N \approx 10^6$ possible bit/spin configurations, but after just 3000 evaluations of (11), many of the lowest minima have apparently had their barriers traversed *en route*. After 300, 1000, and 3000 evaluations, there are respectively 57, 75, and 85 elites (of $L^K = 100$ nominally possible): meanwhile, there are 82 local minima. Many minima have nearest elites with lower values because (e.g.) the minima are in unexplored cells or because a cell contains more than one minimum.

¹⁴NB. For N large, the software described in [99] can be used to generate hard optimization problems similar to (11) with known minima.

¹⁵The barrier tree of a function is a tree whose leaves and internal vertices respectively correspond to local minima and minimal saddles connecting minima [8]. Barrier trees of spin glasses can be efficiently computed using the `barriers` program described in [37] and available at <https://www.tbi.univie.ac.at/RNA/Barriers/>.

6.4 $X = \text{Nondecreasing Bijections on } [0, 1]$

As a penultimate example, we consider a maze-like problem in which we start with a suitable function $f_0 : [0, 1]^2 \rightarrow \mathbb{R}$ and subsequently consider the line integral objective

$$f(\gamma) := \int_{\gamma} f_0 \quad (12)$$

for γ a nondecreasing path from $(0, 0)$ to $(1, 1)$. This problem has several interesting and attractive features:

- it is infinite-dimensional, and any useful discretization is either very high-dimensional or such that the notion of dimension itself is inapplicable to the space X of paths;
- it is maze-like, with multiple local minima, opportunities for “deception,” straightforward visualization, etc.;
- we can use an estimate of f_0 to estimate f in turn;
- the global optimum can be efficiently approximated by computing the shortest path through a weighted DAG (or by dynamic programming *per se*).

A suitable global generator G requires a bit of engineering: uniformly random lattice paths in $(\lambda Z)^2$ from the origin to $(1, 1)$ are easy to construct, but are exponentially concentrated along the diagonal joining the two endpoints, which obstructs exploration. Instead, we take the approach indicated in the left panel of Figure 8, uniformly sampling a point on the diagonal between $(0, 1)$ and $(1, 0)$, then recursively uniformly sampling points on diagonals of rectangles induced by parent points in a binary tree structure. The right panel of Figure 8 shows $L = 15$ landmarks obtained this way with a tree depth of 2, $T = \lceil L \log L \rceil = 41$, and the usual L^2 distance.

The design of a suitable local generator g is also not entirely trivial: it is necessary to preserve the nondecreasing property of paths. For our instantiation, if a path has n waypoints (including the endpoints), then we perform the following procedure $n' := \lceil (n - 2)\theta \rceil$ times: i) we sample from a PDF on the set $\{\text{insert}, \text{move}, \text{delete}\}$ that depends on n' ; ii) according to the sample, we either insert a new waypoint in a rectangle with adjacent waypoints as corners that is subsequently scaled by θ ; delete a waypoint if tenable; or move a waypoint, again in a rectangle with corners determined by adjacent waypoints and subsequently scaled by θ .

Finally, we take f_0 as a weighted sum of 100 Gaussians with uniformly random centers and covariance $10^{-3}I$; the weights are $\sim \mathcal{U}([-1, 1])$. We take $K = 2$, $M = 10000$, and $\mu = 128$. In line with the spirit of our developments, we also estimate (12) by performing a linear RBF interpolation of f_0 using waypoints in paths near the current one. However, we also evaluate f_0 on ≈ 100 points along paths to produce a reasonably accurate value for the objective (12).

The resulting elites are shown in the left panel of Figure 9; the right panel shows all of the waypoints considered along the way. Higher-performing elites are shown in Figure 10. We can see that elites hierarchically coalesce and diverge. Figure 11 shows the 46 (= number of elites) shortest paths through weighted DAGs with edges from $\lambda \cdot (j, k)$ to $\lambda \cdot (j+1, k)$ and $\lambda \cdot (j, k+1)$ for $\lambda \in \{1/10, 1/100\}$ and weights given by $\lambda \cdot f_0(\text{edge midpoint})$; also shown is the closest elite to the shortest path and the elite with the best value of f . Note that although there is an elite that approximates the shortest paths well, none of these paths are close to the high-performing “upper branch” paths shown in Figure 10.

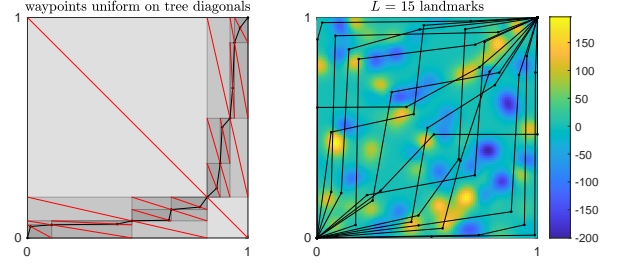


Figure 8: (Left) A path connecting a binary tree of waypoints that are uniformly sampled on diagonals. (Right) Landmarks superimposed on a plot of f_0 .

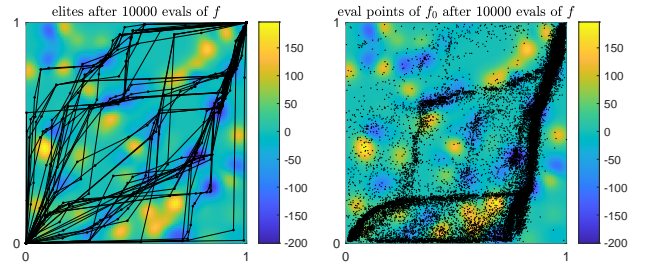


Figure 9: (Left) Elites. (Right) Waypoints on evaluated paths.

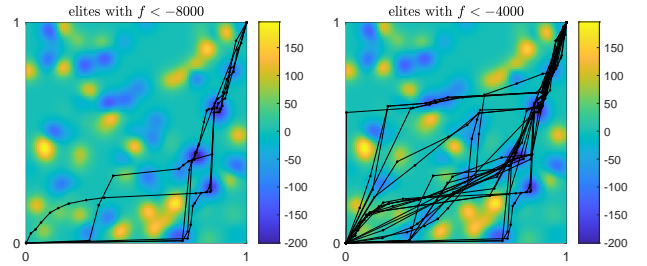


Figure 10: As in the right panel of Figure 9, but for elites with $f < -8000$ (resp., -4000) on the left (resp., right).

6.5 $X = S^{N-1}$

As a final example to further demonstrate the versatility of our approach, we construct and fuzz (i.e., we aim to comprehensively evaluate behavior on the basis of randomly generated inputs to) [13, 79, 123, 126] 100 toy programs that move a unit vector on a high-dimensional sphere $S^{N-1} \subset \mathbb{R}^N$ according to the following procedure:

First, in each case we generate a program “skeleton” using 300 productions from the probabilistic context free grammar [119]

$$S \rightarrow S; S \mid \text{if } b; S; \text{fi} \mid \text{while } b; S; \text{end} \quad (13)$$

where S is shorthand for a line separator: the production probabilities are respectively 0.6, 0.1, and 0.3. The tokens S and b respectively represent statements/subroutines and Boolean predicates.

Second, we form the resulting *control flow graph* (CFG) [27] by associating vertices with lines in the skeleton and edges according

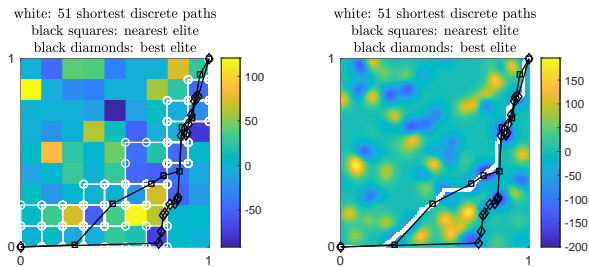


Figure 11: (Left) The 46 (= number of elites) shortest paths (white) through a discrete approximation with $\lambda^{-1} = 10$ subdivisions per dimension and the elites that are closest to the shortest path (black squares) and that are best performing (black diamonds). (Right) As on the left, but with $\lambda^{-1} = 100$.

Table 1: CFG edge: $[\cdot] :=$ line number of matching token.

source at line j	target(\top)	target(\perp)
if b	$j + 1$	[fi]+1
while b	$j + 1$	[end]+1
end	[while]	-
fi or S	$j + 1$	-

to Table 1. Next, we fully instantiate a program by i) replacing a token S on line j of the program by the assignment $x \leftarrow S_j x$, where S_j is a orthogonal matrix of dimension $N = 10$ sampled uniformly at random [112]; and ii) replacing a token b on line k of the program by the predicate $b_k^T x > 0$, where $b_k \sim \mathcal{U}(S^{N-1})$.

Third, we literally draw the CFG using MATLAB’s layered option and define an objective function to be the depth—literally, the least vertical coordinate in the drawing—reached when traversing $2 \max d_{CFG}(\text{START}, \cdot)$ edges in the CFG by dynamically executing the program, where here the program entry and asymmetric digraph distance on the CFG are indicated. The other inputs for the algorithm are mostly familiar from other examples above: $d =$ distance on S^{N-1} (we actually get slightly better results with the ambient Euclidean distance [not shown]); $L = 15$; $T = \lceil L \log L \rceil = 41$; $K = 2$; $G =$ sampling from $\mathcal{U}(S^{N-1})$; $g(\cdot | x, \theta)$ the unit-length normalization of sampling from $\mathcal{N}(x, \theta^2 I)$; $\mu = 128$; and $M = 1000$. Again, we do this for 100 different programs.

In Figure 12 we show two of the 100 examples of “code coverage” using Algorithm 1 *versus* G alone. Although on occasion G produces better coverage by itself, this is comparatively uncommon, as the right panel of Figure 13 illustrates. It is worth noting that the objective here presents some fundamental difficulties for optimization: by construction, it is piecewise constant on intricate regions (see left panel of Figure 13). From this perspective, the mere existence of a clear advantage is significant.

7 “EXTREMAL” DIVERSITY AT SCALE ZERO

In the limit $t \uparrow \infty$, a weighting tends to the vector 1; this and consideration of examples such as in Figure 1 suggest that the opposite limit $t \downarrow 0$ encodes “extremal” information about diversity.

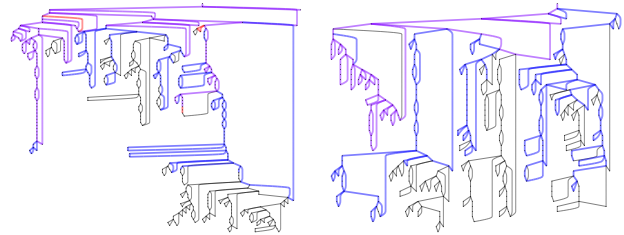


Figure 12: (Left) Coverage for the first of 100 CFGs by Algorithm 1 as described in the text, *versus* by repeatedly executing the global generator G for $M = 1000$ times. Edges exercised only by Algorithm 1 are blue; edges exercised only by G are red; and edges exercised by both are purple. (Right) As in the left panel, but for the last of 100 CFGs.

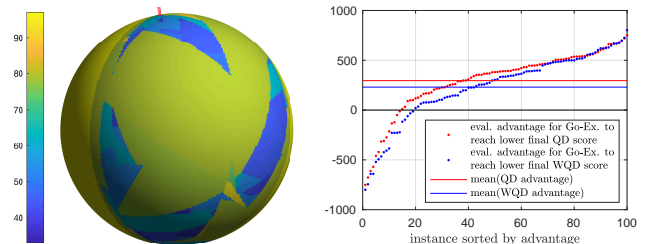


Figure 13: (Left) An objective on S^2 obtained along the same lines as described in §6.5 for S^9 , and evaluated on vertices of a geodesic polyhedron with 163842 vertices. The grid optimum is attained on just eight vertices near the top, indicated with a red marker. (Right) Evaluation advantage of Algorithm 1 relative to the global generator G to reach the lower (W)QD-score achieved by either over the course of $M = 1000$ evaluations. Note that even though about 15-20 percent of instances are disadvantageous, overall there is still a 21-27 percent overall advantage for Algorithm 1. This advantage is significant in light of the objective’s behavior.

Figure 15 shows examples of weightings that maximize diversity at $t = 0$ and compares one of these to the corresponding weighting at $t = t_+$. It is clear that the former dramatically singles out “boundary” points of a sort. In fact for Euclidean examples, modulo a change of metric $d \mapsto \sqrt{d}$ and re-embedding into Euclidean space,¹⁶ such weightings actually single out points lying on a minimal enclosing sphere (see below).

An obvious question is whether or not this extremal notion of diversity can provide an advantage when incorporated into Algorithm 1. However, any possibility of a positive answer to this question requires a reasonably efficient algorithm for actually computing the diversity at $t = 0$. We pursue this first, focusing on the case $q = 1$ as it corresponds most closely to Shannon entropy and turns out to admit an elegant algorithm (recall that the distribution maximizing diversity does not depend on q in the end).

¹⁶See Proposition 4.12 of [31].

For p in the simplex $\Delta_{n-1} := \{p \in [0, 1]^n : 1^T p = 1\}$ of nonnegative probability distributions, the diversity of order 1 is

$$D_1^Z(p) := \prod_{j:p_j>0} (Zp)_j^{-p_j} \quad (14)$$

and the corresponding similarity-sensitive generalization of Shannon entropy is

$$\log D_1^Z(p) = - \sum_{j:p_j>0} p_j \log(Zp)_j. \quad (15)$$

We would like to compute the maximum value of (15) for the common case $Z = \exp[-td]$ in the limit $t \downarrow 0$ for a generic invertible dissimilarity matrix d . While this goal turns out to be overly ambitious in practice, we can still manage fairly well.

The first-order approximation $Z = \exp[-td] \approx 11^T - td$ yields

$$\log D_1^Z(p) \approx tp^T dp. \quad (16)$$

The term $p^T dp$ in the right hand side of (16) is the *quadratic entropy* [101] and the problem of maximizing it over Δ_{n-1} has been considered in, e.g., [52, 59, 60, 98]. In the Euclidean setting, [98] points out that this maximum quadratic entropy is realized by the squared radius of a minimal sphere containing points with distance matrix \sqrt{d} (which is also a Euclidean distance matrix); the support of p corresponds to the subset of points on this sphere.

It can be shown (see, e.g., Example 5.16 of [31]) that maximizing $p^T d' p$ over Δ_{n-1} is NP-hard for arbitrary d' . This is not surprising in light of the fact that quadratic programming is generally NP-hard [106] and remains so even when the underlying matrix has only a single eigenvalue with a given sign [94]. While this sign condition is typical for Euclidean distance matrices [11, 108], it nevertheless turns out that for d a Euclidean distance matrix, $p^T dp$ is convex (see Theorem 4.3 of [102] and Proposition 5.20 of [31]), so it can be efficiently maximized over any sufficiently simple polytope via quadratic programming. More generally, $p^T dp$ is convex if d is *strict negative type*, i.e., $x^T dx < 0$ for $1^T x = 0$: this entails that Z is positive semidefinite for all $t > 0$.¹⁷ In §7.1 we exhibit a more practical algorithm than quadratic programming for maximizing the quadratic entropy of strict negative type metrics.

On the other hand, it appears likely that maximizing $p^T dp$ over Δ_{n-1} is still generally NP-hard when Z is positive definite only for all sufficiently small t . Yet in this intermediate case we can still do better than despairing at general intractability or resorting to Algorithm 4 below as a heuristic of uncertain effectiveness by developing a nontrivial bound. By Theorem 3.2 of [60] we have that

$$\arg \max_{p \in \mathbb{R}^n: 1^T p = 1} p^T dp = \frac{d^{-1}1}{1^T d^{-1}1},$$

though in general this extremum (which also turns out to equal the limiting weighting $\lim_{t \downarrow 0} Z^{-1}1$) will have negative components. Thus the best practical recourse when Z is positive definite only for all sufficiently small t is to bound $p^T dp$ using

$$\max_{p \in \Delta_{n-1}} p^T dp \leq \max_{p \in \mathbb{R}^n: 1^T p = 1} p^T dp = \frac{1}{1^T d^{-1}1}. \quad (17)$$

¹⁷See also [72–74, 82]. Per Lemma 1.7 of [96] as rephrased in Theorem 4.2 of [102], we can encode the truth or falsity of the assertion that a symmetric nonnegative matrix d of size n is negative type (i.e., $x^T dx \leq 0$ for $1^T x = 0$) in one line of MATLAB, viz. `eigs(d(2:n,2:n)-d(2:n,1)-d(1,2:n)+d(1,1),1,'smallestabs')<0`.

This unpacks as

$$\lim_{t \downarrow 0} \frac{\log D_1^Z(p)}{\max_{p \in \Delta_{n-1}} \log D_1^Z(p)} \geq \lim_{t \downarrow 0} \frac{\log D_1^Z(p)}{\max_{p \in \mathbb{R}^n: 1^T p = 1} \log D_1^Z(p)} = (p^T dp) \cdot (1^T d^{-1}1). \quad (18)$$

7.1 Maximizing quadratic entropy of strict negative type metrics

Translated into our context, Proposition 5.20 of [31] states that if d is strict negative type (again, recall this includes Euclidean distance matrices), then

$$p_*(d) := \arg \max_{p \in \Delta_{n-1}} p^T dp \quad (19)$$

is uniquely characterized by the conditions

- i) $p_*(d) \in \Delta_{n-1}$
- ii) $e_j^T dp \geq e_k^T dp$ for all $j \in \text{supp}(p)$ and $k \in [n]$.

The following theorem generalizes Theorem 5.23 of [31] and addresses the $t \downarrow 0$ limit of an algorithm described in the preprint [54] but omitted from the published version of record.

THEOREM 2. *For d strict negative type, Algorithm 4 returns $p_*(d)$ in time $O(n^{\omega+1})$, where $\omega \leq 3$ is the exponent characterizing the complexity of matrix multiplication and inversion as implemented.*

Algorithm 4 SCALEZEROARGMAXDIVERSITY(d)

Require: Strict negative type metric d on $[n]$

- 1: $p \leftarrow \frac{d^{-1}1}{1^T d^{-1}1}$
- 2: **while** $\exists i : p_i < 0$ **do**
- 3: $J \leftarrow \{j : w_j > 0\}$ // Restriction of support
- 4: $p \leftarrow 0_{[n]}$
- 5: $p_J \leftarrow \frac{d_{J,J}^{-1}1_J}{1_J^T d_{J,J}^{-1}1_J}$
- 6: **end while**

Ensure: $p = p_*(d)$

PROOF. First, we show that condition ii) is maintained throughout the while loop of Algorithm 4. Note that the condition trivially holds at initialization, and also note that any nonempty principal submatrix $d_{J,J}$ of d is strict negative type and hence invertible. Block partitioning d and p respectively as

$$d = \begin{pmatrix} d_{J,J} & d_{J,J^c} \\ d_{J^c,J} & d_{J^c,J^c} \end{pmatrix};$$

$$p = p_J \oplus 0_{J^c} = \frac{d_{J,J}^{-1}1_J}{1_J^T d_{J,J}^{-1}1_J} \oplus 0_{J^c},$$

where J^c denotes the set complement $[n] \setminus J$, we obtain

$$dp = \frac{1_J \oplus d_{J^c,J} p_J}{1_J^T d_{J,J}^{-1}1_J}.$$

Thus for $j \in J$

$$e_j^T dp = \frac{1}{1_J^T d_{J,J}^{-1}1_J},$$

and for $k \in J^c$

$$e_k^T dp = \frac{d_{k,J} d_{J,J}^{-1} 1_J}{1_J^T d_{J,J}^{-1} 1_J}.$$

As a result, the case $k \in J$ for condition ii) is trivial, so condition ii) is equivalent to

$$1 \geq d_{k,J} d_{J,J}^{-1} 1_J$$

for all $k \in J^c$. We rewrite the right hand side until the satisfaction of condition ii)'s equivalent becomes obvious:

$$\begin{aligned} d_{k,J} d_{J,J}^{-1} 1_J &= \sum_{j' \in J} \sum_{j \in J} d_{kj} (d^{-1})_{jj'} \\ &= \sum_{j' \in J} (d d^{-1})_{kj'} \\ &= \sum_{j' \in J} \delta_{kj'} \\ &= 0 \end{aligned}$$

where the last equality is because $k \in J^c$.

Algorithm 4 halts once condition i) holds. Finally, because the while loop takes at most n iterations, the computational complexity bound follows. \square

COROLLARY 1. For d strict negative type, Algorithm 4 efficiently computes $\arg \max_{p \in \Delta_{n-1}} \lim_{t \downarrow 0} D_q^Z(p)$ for all q .

7.2 Practicalities and examples

As a practical matter, we have found that Algorithm 4 also performs better than a quadratic programming solver: it is much faster (in MATLAB on ≈ 1000 points, a few hundredths of a second versus several seconds for a quadratic programming solver with tolerance 10^{-10}) and more accurate, in particular by handling sparsity exactly. Figure 15 shows representative results. It is also very simple to implement: excepting any preliminary checks on inputs, each line of the algorithm can be (somewhat wastefully) implemented in a standard-length line of MATLAB.

7.3 Incorporating diversity contributions at scale zero and/or a fuzzing-inspired exploration effort into Algorithm 1

There are two obvious places to incorporate scale zero computations into Algorithm 1: on elites, and on probes/expeditions sent from elites. These respectively address the core “go” and “explore” mechanisms in our approach. We modified our original implementation to support both of these as options, along with the “entropic power schedule” of [12] as an option to govern the exploration effort.

Perhaps surprisingly, applying these options to the Rastrigin function indicates that none of them has a positive effect, as Figure 15 illustrates (we do not show the entropic power schedule variant as it was computed for fewer function evaluations and its poor performance was already evident). The poor performance of scale zero options appears to be because they respectively suppress exploration around “interior” elites and near elites generically for the cases in which the scale zero options are applied to elites

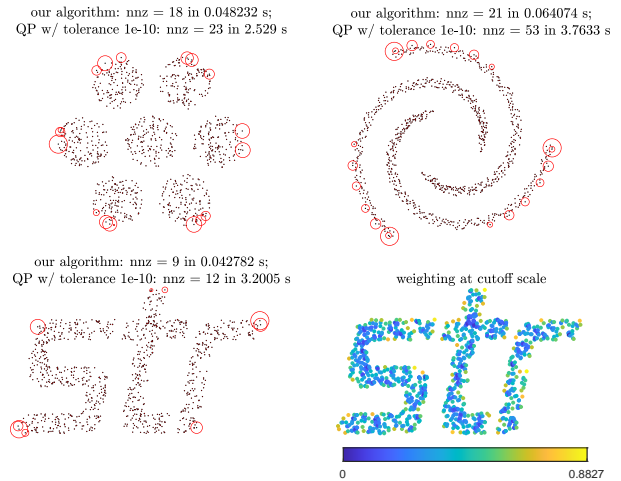


Figure 14: (Upper left, upper right, and lower left) Outputs of Algorithm 4 on the Euclidean distance matrix of the ≈ 1000 black points, indicated by red circles with radius proportional to the corresponding entries of p . The numbers of nonzero (nnz) entries of the output are indicated along with the run-times of the algorithm; the same numbers are reported for a quadratic programming run with tolerance 10^{-10} . (Lower right) The weighting on the same points as in the lower left panel at the strong cutoff $t = t_+$. Recall that this scale is the least such that the weighting is nonnegative. Note that even at this scale, weighting components still tend to be at corners or at least boundaries.

and probes/expeditions. These factors in turn both impact the ability of corresponding variants of Algorithm 1 to find high-quality solutions.

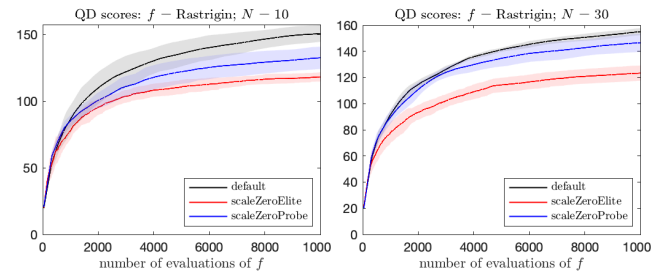


Figure 15: (Left) QD-scores for variants of Algorithm 4 using scale zero constructions and applied to the Rastrigin function in dimension $N = 10$ (cf. Figure 6). Algorithm 4 itself, indicated as the default here, clearly outperforms its variants. (Right) As in the left panel, but for dimension $N = 30$.

Our consideration of the entropic power schedule of [12] was inspired by our development of a cousin of Algorithm 1 for the fuzzing problem (see §6.5), where we confirmed it offered leading performance in accordance with theoretical arguments behind it (details will be reported elsewhere). However, the underlying rationale of this construction is mismatched with typical considerations

of QD algorithms *per se* to a degree that was only obvious to us after doing an experiment.

In the fuzzing problem, improving an input amounts to identifying an essentially new part of the behavior space. Doing the latter optimally is precisely the aim of the entropic power schedule. Meanwhile, the idea permeating much of the present paper of modeling an objective is fundamentally ill-posed in the context of fuzzing: once a program’s behavior is reasonably well understood in a neighborhood of a given input, that input should be ignored in favor of others whose local behavior is not yet well understood.

In short, while we believe a variant of Algorithm 1 can improve the state of the art for fuzzing, and ideas from both diversity optimization at scale zero and fuzzing and are relevant to quality-diversity, a naive transplantation of ideas is inadequate in either direction. Finally, combining these ideas will also require some combination of delicacy and/or approximation. If d is strict negative type, we can resort to Algorithm 4 as in applications of Go-Explore that seek to interpolate an objective on Euclidean space. However, for typical fuzzing applications, we must resort to the bound (18) to govern a power schedule of our fuzzer at scale $t = 0$.¹⁸

8 CONCLUSION

Our formulation of Go-Explore illustrates that a single quality-diversity algorithm can be applied across very general settings. The algorithm centers on a mathematically principled definition of diversity that admits a tractable maximization scheme. The algorithm usefully separates concerns of problem details, surrogate construction, and its core quality-diversity mechanisms.

Although we focused here on very structured input spaces in order to produce efficient surrogates for expensive objectives in the context of quality-diversity algorithms, the notions of diversity, magnitude, and weightings provide tools for building optimization algorithms more generally. In particular, the prospect of using neural surrogates and/or methods for accelerating the computation of weightings such as [26, 104] suggest wider scope for applications.

Finally, while the results of §7 do not yield improvements to Algorithm 1, we believe they are of independent interest and can yield useful applications of their own.

ACKNOWLEDGMENTS

Thanks to Zac Hoffman and Rachelle Horwitz-Martin for clarifying questions and suggestions, and to Karel Devriendt for an illuminating discussion about maximizing quadratic entropy. This research was developed with funding from the Defense Advanced Research Projects Agency (DARPA). The views, opinions and/or findings expressed are those of the author and should not be interpreted as representing the official views or policies of the Department of Defense or the U.S. Government. Distribution Statement “A” (Approved for Public Release, Distribution Unlimited).

REFERENCES

- [1] 1981. RFC791: Internet protocol.
- [2] Divesh Aggarwal, Daniel Dadush, Oded Regev, and Noah Stephens-Davidowitz. 2015. Solving the shortest vector problem in $2n$ time using discrete Gaussian sampling. In *Proceedings of the forty-seventh annual ACM symposium on Theory of computing*. 733–742.

- [3] Daniele Agostini and Carlos Améndola. 2019. Discrete Gaussian distributions via theta functions. *SIAM Journal on Applied Algebra and Geometry* 3, 1 (2019), 1–30.
- [4] Giuseppe Amato and Pasquale Savino. 2008. Approximate similarity search in metric spaces using inverted files. In *Proceedings of the 3rd international conference on Scalable information systems*. Citeseer, 1–10.
- [5] Emmanuelle Anceaume, Yann Busnel, and Bruno Sericola. 2015. New results on a generalized coupon collector problem using Markov chains. *Journal of Applied Probability* 52, 2 (2015), 405–418.
- [6] Dana Angluin. 1987. Learning regular sets from queries and counterexamples. *Information and computation* 75, 2 (1987), 87–106.
- [7] Mikhail Auguston, James Bret Michael, and Man-Tak Shing. 2005. Environment behavior models for scenario generation and testing automation. *ACM SIGSOFT Software Engineering Notes* 30, 4 (2005), 1–6.
- [8] Oren M Becker and Martin Karplus. 1997. The topology of multidimensional potential energy surfaces: Theory and application to peptide structure and kinetics. *The Journal of chemical physics* 106, 4 (1997), 1495–1517.
- [9] Jakob Bernasconi. 1987. Low autocorrelation binary sequences: statistical mechanics and configuration space analysis. *Journal de Physique* 48, 4 (1987), 559–567.
- [10] Avrim Blum, John Hopcroft, and Ravindran Kannan. 2020. *Foundations of data science*. Cambridge University Press.
- [11] E Bogomolny, O Bohigas, and C Schmit. 2007. Distance matrices and isometric embeddings. *arXiv preprint arXiv:0710.2063* (2007).
- [12] Marcel Böhme, Valentin JM Manès, and Sang Kil Cha. 2020. Boosting fuzzer efficiency: An information theoretic perspective. In *Proceedings of the 28th ACM Joint Meeting on European Software Engineering Conference and Symposium on the Foundations of Software Engineering*. 678–689.
- [13] Marcel Böhme, Van-Thuan Pham, Manh-Dung Nguyen, and Abhik Roychoudhury. 2017. Directed greybox fuzzing. In *Proceedings of the 2017 ACM SIGSAC Conference on Computer and Communications Security*. 2329–2344.
- [14] Erwin Bolthausen and Anton Bovier. 2007. *Spin glasses*. Springer.
- [15] Jean Bourgain. 1985. On Lipschitz embedding of finite metric spaces in Hilbert space. *Israel Journal of Mathematics* 52, 1 (1985), 46–52.
- [16] RT Braden, DA Borman, and C Partridge. 1988. RFC1071: Computing the internet checksum.
- [17] Steven P Brady, Daniel I Bolnick, Amy L Angert, Andrew Gonzalez, Rowan DH Barrett, Erika Crispo, Alison M Derry, Christopher G Eckert, Dylan J Fraser, Gregor F Fussmann, et al. 2019. Causes of maladaptation. *Evolutionary Applications* 12, 7 (2019), 1229–1242.
- [18] Janez Brest and Borko Bošković. 2021. Low Autocorrelation Binary Sequences: Best-Known Peak Sidelobe Level Values. *IEEE Access* 9 (2021), 67713–67723.
- [19] Martin D Buhmann. 2003. *Radial basis functions: theory and implementations*. Cambridge University Press.
- [20] Eric Bunch, Daniel Dickinson, Jeffery Kline, and Glenn Fung. 2020. Practical applications of metric space magnitude and weighting vectors. *arXiv preprint arXiv:2006.14063* (2020).
- [21] Eric Bunch, Jeffery Kline, Daniel Dickinson, Suhaas Bhat, and Glenn Fung. 2021. Weighting vectors for machine learning: numerical harmonic analysis applied to boundary detection. *arXiv preprint arXiv:2106.00827* (2021).
- [22] Leo Cazenille. 2019. Comparing reliability of grid-based Quality-Diversity algorithms using artificial landscapes. In *Proceedings of the Genetic and Evolutionary Computation Conference Companion*. 249–250.
- [23] Timothy M Chan and Mihai Pătraşcu. 2010. Counting inversions, offline orthogonal range counting, and related problems. In *Proceedings of the twenty-first annual ACM-SIAM symposium on Discrete Algorithms*. SIAM, 161–173.
- [24] Konstantinos Chatzilygeroudis, Antoine Cully, Vassilis Vassiliades, and Jean-Baptiste Mouret. 2021. Quality-Diversity Optimization: a novel branch of stochastic optimization. In *Black Box Optimization, Machine Learning, and No-Free Lunch Theorems*. Springer, 109–135.
- [25] Edgar Chávez, Karina Figueroa, and Gonzalo Navarro. 2008. Effective proximity retrieval by ordering permutations. *IEEE Transactions on Pattern Analysis and Machine Intelligence* 30, 9 (2008), 1647–1658.
- [26] D Yu Chenhan, William B March, and George Biros. 2017. An $n \log n$ parallel fast direct solver for kernel matrices. In *2017 IEEE International Parallel and Distributed Processing Symposium (IPDPS)*. IEEE, 886–896.
- [27] Keith D Cooper and Linda Torczon. 2011. *Engineering a compiler*. Elsevier.
- [28] David Corfield, Hisham Sati, and Urs Schreiber. 2021. Fundamental weight systems are quantum states. *arXiv preprint arXiv:2105.02871* (2021).
- [29] Zoe Cournia, Bryce K Allen, Thijs Beuming, David A Pearlman, Brian K Radak, and Woody Sherman. 2020. Rigorous free energy simulations in virtual screening. *Journal of Chemical Information and Modeling* 60, 9 (2020), 4153–4169.
- [30] Antoine Cully. 2021. Multi-emitter MAP-elites: improving quality, diversity and data efficiency with heterogeneous sets of emitters. In *Proceedings of the Genetic and Evolutionary Computation Conference*. 84–92.
- [31] Karel Devriendt. 2022. *Graph geometry from effective resistances*. Ph.D. Dissertation. University of Oxford.

¹⁸Proposition 5.17 of [31] gives the generic bounds $p^T dp \in [\frac{1}{2}, \frac{n-1}{n}] \cdot \max_{jk} d_{jk}$.

- [32] Carola Doerr, Furong Ye, Naama Horesh, Hao Wang, Ofer M Shir, and Thomas Bäck. 2020. Benchmarking discrete optimization heuristics with IOHprofiler. *Applied Soft Computing* 88 (2020), 106027.
- [33] Adrien Ecoffet, Joost Huizinga, Joel Lehman, Kenneth O Stanley, and Jeff Clune. 2021. First return, then explore. *Nature* 590, 7847 (2021), 580–586.
- [34] Ronald Fagin, Ravi Kumar, and Dakshinamurthi Sivakumar. 2003. Comparing top k lists. *SIAM Journal on discrete mathematics* 17, 1 (2003), 134–160.
- [35] Fernando F Ferreira, José F Fontanari, and Peter F Stadler. 2000. Landscape statistics of the low-autocorrelation binary string problem. *Journal of Physics A: Mathematical and General* 33, 48 (2000), 8635.
- [36] Philippe Flajolet, Daniele Gardy, and Loÿs Thimonier. 1992. Birthday paradox, coupon collectors, caching algorithms and self-organizing search. *Discrete Applied Mathematics* 39, 3 (1992), 207–229.
- [37] Christoph Flamm, Ivo L. Hofacker, Peter F. Stadler, and Michael T. Wolfinger. 2002. Barrier Trees of Degenerate Landscapes. 216, 2 (2002), 155–155. <https://doi.org/doi:10.1524/zpch.2002.216.2.155>
- [38] Matthew C Fontaine, Ruilin Liu, Ahmed Khalifa, Jignesh Modi, Julian Togelius, Amy K Hoover, and Stefanos Nikolaidis. 2021. Illuminating mario scenes in the latent space of a generative adversarial network. In *Proceedings of the AAAI Conference on Artificial Intelligence*, Vol. 35. 5922–5930.
- [39] Matthew C Fontaine and Stefanos Nikolaidis. 2021. Evaluating Human-Robot Interaction Algorithms in Shared Autonomy via Quality Diversity Scenario Generation. *ACM Transactions on Human-Robot Interaction* (2021).
- [40] Matthew C Fontaine, Julian Togelius, Stefanos Nikolaidis, and Amy K Hoover. 2020. Covariance matrix adaptation for the rapid illumination of behavior space. In *Proceedings of the 2020 genetic and evolutionary computation conference*. 94–102.
- [41] José F Fontanari and Peter F Stadler. 2002. Fractal geometry of spin-glass models. *Journal of Physics A: Mathematical and General* 35, 7 (2002), 1509.
- [42] Adam Gaier, Alexander Asteroth, and Jean-Baptiste Mouret. 2018. Data-efficient design exploration through surrogate-assisted illumination. *Evolutionary computation* 26, 3 (2018), 381–410.
- [43] Adam Gaier, Alexander Asteroth, and Jean-Baptiste Mouret. 2020. Discovering representations for black-box optimization. In *Proceedings of the 2020 Genetic and Evolutionary Computation Conference*. 103–111.
- [44] Kyle Yingkai Gao, Achille Fokoue, Heng Luo, Arun Iyengar, Sanjoy Dey, and Ping Zhang. 2018. Interpretable drug target prediction using deep neural representation. In *Proceedings of the 27th International Joint Conference on Artificial Intelligence*. 3371–3377.
- [45] Heiko Gimperlein and Magnus Goffeng. 2021. On the magnitude function of domains in Euclidean space. *American Journal of Mathematics* 143, 3 (2021), 939–967.
- [46] Aristides Gionis, Piotr Indyk, Rajeev Motwani, et al. 1999. Similarity search in high dimensions via hashing. In *Vldb*, Vol. 99. 518–529.
- [47] Marzia M Giuliani, Jeannette Adu-Bobie, Maurizio Comanducci, Beatrice Aricò, Silvana Savino, Laura Santini, Brunella Brunelli, Stefania Bambini, Alessia Biolchi, Barbara Capocchi, et al. 2006. A universal vaccine for serogroup B meningococcus. *Proceedings of the National Academy of Sciences* 103, 29 (2006), 10834–10839.
- [48] Rafael Gómez-Bombarelli, Jorge Aguilera-Iparraguirre, Timothy D Hirzel, David Duvenaud, Dougal Maclaurin, Martin A Blood-Forsythe, Hyun Sik Chae, Markus Einzinger, Dong-Gwang Ha, Tony Wu, et al. 2016. Design of efficient molecular organic light-emitting diodes by a high-throughput virtual screening and experimental approach. *Nature materials* 15, 10 (2016), 1120–1127.
- [49] Joseph Grinnell. 1924. Geography and evolution. *Ecology* 5, 3 (1924), 225–229.
- [50] Zhaohan Daniel Guo, Mohammad Gheshlaghi Azar, Alaa Saade, Shantanu Thakoor, Bilal Piot, Bernardo Avila Pires, Michal Valko, Thomas Mesnard, Tor Lattimore, and Rémi Munos. 2021. Geometric entropic exploration. *arXiv preprint arXiv:2101.02055* (2021).
- [51] Nikolaus Hansen. 2016. The CMA evolution strategy: A tutorial. *arXiv preprint arXiv:1604.00772* (2016).
- [52] Poul Hjørth, Petr Lisoněk, Steen Markvorsen, and Carsten Thomassen. 1998. Finite metric spaces of strictly negative type. *Linear algebra and its applications* 270, 1-3 (1998), 255–273.
- [53] Zachary Hoffman and Steve Huntsman. 2022. Benchmarking an algorithm for expensive high-dimensional objectives on the bbob and bbob-largescale testbeds. In *GECCO Workshop on Black-Box Optimization Benchmarking (BBOB 2022)*.
- [54] Steve Huntsman. 2022. Diversity enhancement via magnitude. *arXiv preprint arXiv:2201.10037* (2022).
- [55] Steve Huntsman. 2022. Parallel black-box optimization of expensive high-dimensional multimodal functions via magnitude. *arXiv preprint arXiv:2201.11677* (2022).
- [56] Steve Huntsman. 2023. Quality-diversity in dissimilarity spaces. In *Proceedings of the Genetic and Evolutionary Computation Conference*. 1009–1018.
- [57] Steve Huntsman and Arman Rezaee. 2015. De Bruijn entropy and string similarity. In *WORDS*.
- [58] Piotr Indyk and Rajeev Motwani. 1998. Approximate nearest neighbors: towards removing the curse of dimensionality. In *Proceedings of the thirtieth annual ACM symposium on Theory of computing*. 604–613.
- [59] János Izsák and László Szeidl. 2002. Quadratic diversity: its maximization can reduce the richness of species. *Environmental and Ecological Statistics* 9 (2002), 423–430.
- [60] Saichi Izumino and Noboru Nakamura. 2006. Maximization of quadratic forms expressed by distance matrices. *Hokkaido Mathematical Journal* 35, 3 (2006), 641–658.
- [61] Guha Jayachandran, Michael R Shirts, Sanghyun Park, and Vijay S Pande. 2006. Parallelized-over-parts computation of absolute binding free energy with docking and molecular dynamics. *The Journal of chemical physics* 125, 8 (2006), 084901.
- [62] Yunlong Jiao and Jean-Philippe Vert. 2015. The Kendall and Mallows kernels for permutations. In *International Conference on Machine Learning*. PMLR, 1935–1944.
- [63] John Junger, Richard Evans, Alexander Pritzel, Tim Green, Michael Figurnov, Olaf Ronneberger, Kathryn Tunyasuvunakool, Russ Bates, Augustin Židek, Anna Potapenko, et al. 2021. Highly accurate protein structure prediction with AlphaFold. *Nature* 596, 7873 (2021), 583–589.
- [64] Byungkon Kang and Kyomin Jung. 2012. Robust and efficient locality sensitive hashing for nearest neighbor search in large data sets. In *NIPS Workshop on Big Learning (BigLearn), Lake Tahoe, Nevada*. Citeseer, 1–8.
- [65] Mostafa Karimi, Di Wu, Zhangyang Wang, and Yang Shen. 2019. DeepAffinity: interpretable deep learning of compound–protein affinity through unified recurrent and convolutional neural networks. *Bioinformatics* 35, 18 (2019), 3329–3338.
- [66] Paul Kent and Juergen Branke. 2020. Bop-elites, a bayesian optimisation algorithm for quality-diversity search. *arXiv preprint arXiv:2005.04320* (2020).
- [67] Wayne C Koff and Seth F Berkley. 2021. A universal coronavirus vaccine. , 759–759 pages.
- [68] Philip Koopman. 2002. 32-bit cyclic redundancy codes for internet applications. In *Proceedings International Conference on Dependable Systems and Networks*. IEEE, 459–468.
- [69] Andreas Krause and Daniel Golovin. 2014. Submodular function maximization. *Tractability* 3 (2014), 71–104.
- [70] Ravi Kumar and Sergei Vassilvitskii. 2010. Generalized distances between rankings. In *Proceedings of the 19th international conference on World wide web*. 571–580.
- [71] Joel Lehman and Kenneth O Stanley. 2011. Evolving a diversity of virtual creatures through novelty search and local competition. In *Proceedings of the 13th annual conference on Genetic and evolutionary computation*. 211–218.
- [72] Tom Leinster. 2021. *Entropy and Diversity: The Axiomatic Approach*. Cambridge University Press.
- [73] Tom Leinster and Christina A Cobbold. 2012. Measuring diversity: the importance of species similarity. *Ecology* 93, 3 (2012), 477–489.
- [74] Tom Leinster and Mark W Meckes. 2016. Maximizing diversity in biology and beyond. *Entropy* 18, 3 (2016), 88.
- [75] Thomas Leinster and Mark W Meckes. 2017. The magnitude of a metric space: from category theory to geometric measure theory. In *Measure Theory in Non-Smooth Spaces*. De Gruyter Open, 156–193.
- [76] Jure Leskovec, Anand Rajaraman, and Jeffrey David Ullman. 2020. *Mining of massive data sets*. Cambridge university press.
- [77] Xiaoyi Li. 2020. A Scenario-Based Development Framework for Autonomous Driving. *arXiv preprint arXiv:2011.01439* (2020).
- [78] Nathan Linial, Eran London, and Yuri Rabinovich. 1995. The geometry of graphs and some of its algorithmic applications. *Combinatorica* 15, 2 (1995), 215–245.
- [79] Valentin JM Manès, HyungSeok Han, Choongwoo Han, Sang Kil Cha, Manuel Egele, Edward J Schwartz, and Maverick Woo. 2019. The art, science, and engineering of fuzzing: A survey. *IEEE Transactions on Software Engineering* 47, 11 (2019), 2312–2331.
- [80] Glenn Martin, Sae Schatz, Clint Bowers, Charles E Hughes, Jennifer Fowlkes, and Denise Nicholson. 2009. Automatic scenario generation through procedural modeling for scenario-based training. In *Proceedings of the Human Factors and Ergonomics Society Annual Meeting*, Vol. 53. SAGE Publications Sage CA: Los Angeles, CA, 1949–1953.
- [81] Andrew T McNutt, Paul Francoeur, Rishal Aggarwal, Tomohide Masuda, Rocco Meli, Matthew Ragoza, Jocelyn Sunseri, and David Ryan Koes. 2021. GNINA 1.0: molecular docking with deep learning. *Journal of cheminformatics* 13, 1 (2021), 1–20.
- [82] Mark W Meckes. 2013. Positive definite metric spaces. *Positivity* 17, 3 (2013), 733–757.
- [83] Mark W Meckes. 2015. Magnitude, diversity, capacities, and dimensions of metric spaces. *Potential Analysis* 42, 2 (2015), 549–572.
- [84] Andrea Montanari. 2021. Optimization of the Sherrington–Kirkpatrick Hamiltonian. *SIAM J. Comput.* 0 (2021), FOCS19–1.

- [85] Todd K Moon. 2020. *Error correction coding: mathematical methods and algorithms*. John Wiley & Sons.
- [86] David M Morens, Jeffery K Taubenberger, and Anthony S Fauci. 2022. Universal coronavirus vaccines—an urgent need. *New England Journal of Medicine* 386, 4 (2022), 297–299.
- [87] Jean-Baptiste Mouret and Jeff Clune. 2015. Illuminating search spaces by mapping elites. *arXiv preprint arXiv:1504.04909* (2015).
- [88] George L Nemhauser, Laurence A Wolsey, and Marshall L Fisher. 1978. An analysis of approximations for maximizing submodular set functions—I. *Mathematical programming* 14, 1 (1978), 265–294.
- [89] Anh Mai Nguyen, Jason Yosinski, and Jeff Clune. 2015. Innovation engines: Automated creativity and improved stochastic optimization via deep learning. In *Proceedings of the 2015 Annual Conference on Genetic and Evolutionary Computation*. 959–966.
- [90] David Novak, Martin Kyselak, and Pavel Zezula. 2010. On locality-sensitive indexing in generic metric spaces. In *Proceedings of the Third International Conference on Similarity Search and Applications*. 59–66.
- [91] Hakime Öztürk, Elif Ozkirimli, and Arzuhan Özgür. 2016. A comparative study of SMILES-based compound similarity functions for drug-target interaction prediction. *BMC bioinformatics* 17, 1 (2016), 1–11.
- [92] Tom Packebusch and Stephan Mertens. 2016. Low autocorrelation binary sequences. *Journal of Physics A: Mathematical and Theoretical* 49, 16 (2016), 165001.
- [93] Dmitry Panchenko. 2012. The Sherrington-Kirkpatrick model: an overview. *Journal of Statistical Physics* 149, 2 (2012), 362–383.
- [94] Panos M Pardalos and Stephen A Vavasis. 1991. Quadratic programming with one negative eigenvalue is NP-hard. *Journal of Global optimization* 1, 1 (1991), 15–22.
- [95] Norbert Pardi, Michael J Hogan, Frederick W Porter, and Drew Weissman. 2018. mRNA vaccines—a new era in vaccinology. *Nature reviews Drug discovery* 17, 4 (2018), 261–279.
- [96] K R Parthasarathy and K Schmidt. 1972. *Positive Definite Kernels, Continuous Tensor Products, and Central Limit Theorems of Probability Theory*. Springer.
- [97] Catharine I Paules, Sheena G Sullivan, Kanta Subbarao, and Anthony S Fauci. 2018. Chasing seasonal influenza—the need for a universal influenza vaccine. *New England Journal of Medicine* 378, 1 (2018), 7–9.
- [98] Sandrine Pavoine, Sébastien Ollier, and Dominique Pontier. 2005. Measuring diversity from dissimilarities with Rao’s quadratic entropy: Are any dissimilarities suitable? *Theoretical population biology* 67, 4 (2005), 231–239.
- [99] Dilina Perera, Inimfon Akpabio, Firas Hamze, Salvatore Mandra, Nathan Rose, Maliheh Aramon, and Helmut G Katzgraber. 2020. Chook—A comprehensive suite for generating binary optimization problems with planted solutions. *arXiv preprint arXiv:2005.14344* (2020).
- [100] Justin K Pugh, Lisa B Soros, and Kenneth O Stanley. 2016. Quality diversity: A new frontier for evolutionary computation. *Frontiers in Robotics and AI* 3 (2016), 40.
- [101] C Radhakrishna Rao. 1982. Diversity and dissimilarity coefficients: a unified approach. *Theoretical population biology* 21, 1 (1982), 24–43.
- [102] C Radhakrishna Rao. 1984. Convexity properties of entropy functions and analysis of diversity. *Lecture Notes-Monograph Series* (1984), 68–77.
- [103] Michael S Rosenberg. 2009. *Sequence alignment: methods, models, concepts, and strategies*. Univ of California Press.
- [104] François-Henry Rouet, Xiaoye S Li, Pieter Ghysels, and Artem Napov. 2016. A distributed-memory package for dense hierarchically semi-separable matrix computations using randomization. *ACM Transactions on Mathematical Software (TOMS)* 42, 4 (2016), 1–35.
- [105] Kunal Roy, Supratik Kar, and Rudra Narayan Das. 2015. *A primer on QSAR/QSPR modeling: fundamental concepts*. Springer.
- [106] Sartaj Sahni. 1974. Computationally related problems. *SIAM Journal on computing* 3, 4 (1974), 262–279.
- [107] Soumitra Samanta, Steve O’Hagan, Neil Swainston, Timothy J Roberts, and Douglas B Kell. 2020. VAE-Sim: a novel molecular similarity measure based on a variational autoencoder. *Molecules* 25, 15 (2020), 3446.
- [108] Isaac J Schoenberg. 1937. On certain metric spaces arising from Euclidean spaces by a change of metric and their imbedding in Hilbert space. *Annals of mathematics* (1937), 787–793.
- [109] Bonggun Shin, Sungsoo Park, Keunsoo Kang, and Joyce C Ho. 2019. Self-attention based molecule representation for predicting drug-target interaction. In *Machine Learning for Healthcare Conference*. PMLR, 230–248.
- [110] Eliezer Silva, Thiago Teixeira, George Teodoro, and Eduardo Valle. 2014. Large-scale distributed locality-sensitive hashing for general metric data. In *International Conference on Similarity Search and Applications*. Springer, 82–93.
- [111] Andrew R Solow and Stephen Polasky. 1994. Measuring biological diversity. *Environmental and Ecological Statistics* 1, 2 (1994), 95–103.
- [112] Gilbert W Stewart. 1980. The efficient generation of random orthogonal matrices with an application to condition estimators. *SIAM J. Numer. Anal.* 17, 3 (1980), 403–409.
- [113] Martin Stigge, Henryk Plötz, Wolf Müller, and Jens-Peter Redlich. 2006. *Reversing CRC – theory and practice*. Technical Report SAR-PR-2006-05. Humboldt Universität zu Berlin.
- [114] Eric Sadit Tellez and Edgar Chavez. 2010. On locality sensitive hashing in metric spaces. In *Proceedings of the Third International Conference on Similarity Search and Applications*. 67–74.
- [115] Sibel Toprak, Arne Wichmann, and Sibylle Schupp. 2014. Lightweight structured visualization of assembler control flow based on regular expressions. In *2014 Second IEEE Working Conference on Software Visualization*. IEEE, 97–106.
- [116] Johnny van Doorn, Michael Lee, and Holly Westfall. 2021. Using the weighted Kendall Distance to analyze rank data in psychology. (2021).
- [117] Mihaly Varadi, Stephen Anyango, Mandar Deshpande, Sreenath Nair, Cindy Natassia, Galabina Yordanova, David Yuan, Oana Stroe, Gemma Wood, Agata Laydon, et al. 2022. AlphaFold Protein Structure Database: massively expanding the structural coverage of protein-sequence space with high-accuracy models. *Nucleic acids research* 50, D1 (2022), D439–D444.
- [118] Vassilis Vassiliades, Konstantinos Chatzilygeroudis, and Jean-Baptiste Mouret. 2017. Using centroidal voronoi tessellations to scale up the multidimensional archive of phenotypic elites algorithm. *IEEE Transactions on Evolutionary Computation* 22, 4 (2017), 623–630.
- [119] Nikita Visnevski, Vikram Krishnamurthy, Alex Wang, and Simon Haykin. 2007. Syntactic modeling and signal processing of multifunction radars: A stochastic context-free grammar approach. *Proc. IEEE* 95, 5 (2007), 1000–1025.
- [120] David Weininger. 1988. SMILES, a chemical language and information system. 1. Introduction to methodology and encoding rules. *Journal of chemical information and computer sciences* 28, 1 (1988), 31–36.
- [121] Simon Willerton. 2009. Heuristic and computer calculations for the magnitude of metric spaces. *arXiv preprint arXiv:0910.5500* (2009).
- [122] Feng Xia, Ke Sun, Shuo Yu, Abdul Aziz, Liangtian Wan, Shirui Pan, and Huan Liu. 2021. Graph learning: A survey. *IEEE Transactions on Artificial Intelligence* 2, 2 (2021), 109–127.
- [123] Andreas Zeller, Rahul Gopinath, Marcel Böhme, Gordon Fraser, and Christian Holler. 2019. *The fuzzing book*.
- [124] Yulun Zhang, Matthew Christopher Fontaine, Amy K Hoover, and Stefanos Nikolaidis. 2022. DSA-ME: Deep Surrogate Assisted MAP-Elites. In *ICLR Workshop on Agent Learning in Open-Endedness*.
- [125] Qing Zhou and Wing Hung Wong. 2009. Energy landscape of a spin-glass model: exploration and characterization. *Physical Review E* 79, 5 (2009), 051117.
- [126] Xiaogang Zhu, Sheng Wen, Seyit Camtepe, and Yang Xiang. 2022. Fuzzing: a survey for roadmap. *ACM Computing Surveys (CSUR)* (2022).

A OVERVIEW OF APPENDICES

- §B sketches alternative “go” mechanisms.
- §C details bounds governing “how often to go.”
- §D elaborates on bandwidth in \mathbb{R}^N .
- §E sketches alternative “explore” mechanisms.
- §F lists pseudocode for a baseline version of Go-Explore used in §6.1.1.
- §G shows additional results for §6.2.
- §H details another example over \mathbb{Z}^N involving regular expression matching.
- §I elaborates on the binary example in the main text and details other examples.
- §J addresses the repair and consequent effects of a minor bug in §K.1.
- §K contains source code.

B ALTERNATIVE TECHNIQUES FOR GOING

Alternatives to a distribution on elites would be distributions on all evaluated states or on all cells. Because the number of evaluated states grows linearly, the cubic complexity of standard linear algebra on them can become untenable, so we do not elaborate on the former alternative here.¹⁹

¹⁹Appendix E of [55] discusses how to improve performance for (3): see also §4 of [21].

B.1 Distributions on all cells

A distribution on cells could aim to incorporate i) a weighting based on the underlying dissimilarity d and ii) a global estimate of the objective f . Since §5.2 largely addresses ii), we focus here on i).²⁰

An interesting idea is to use a distance on permutations to define a suitable probability distribution over all cells. Such distances can yield simple positive definite kernels that elegantly dovetail with the magnitude [72] framework. For example, if d is the so-called *Kendall tau/bubble sort* (resp., *Cayley*) distance on S_n that counts the number of transpositions of adjacent (resp., generic) elements needed to transform between two permutations, then the corresponding *Mallows* (resp., *Cayley*) kernel $\exp[-td]$ is positive definite for all $t \geq 0$ [62] (resp., for $t > \log(n-1)$) [28]. The Kendall tau distance can be computed in quasilinear time [23] and the Cayley distance in linear time (by counting cycles in the quotient permutation).

However, there is not much point in pursuing this idea without a mechanism for generating states in cells on demand (necessary in general due to the curse of dimensionality). For $X = \mathbb{R}^N$ the state generation mechanism can be effected using linear programming, but for $X = \mathbb{Z}^N$ integer programming is required, and this may be prohibitively difficult.²¹ For other spaces there may not be a suitable state generation mechanism at all.

Moreover, if we do not incorporate d into the generalized Kendall or Cayley distance, symmetry just leads to a uniform weighting on cells (some of which might also conceivably be degenerate), which will not be adequate for the purpose of promoting diversity beyond the generation of landmarks. While for the ordinary Kendall distance the corresponding similarity matrix (viz., the so-called *Mallows kernel*) is positive definite for any scale [62], the analogous statement for a generalization along the lines of [70] would have to be established (or worked around by operating at scale t_+). See also [34, 116] for other relevant practicalities in this context.

C HOW OFTEN TO GO

Given a distribution p on elites, we want to sample from p often enough so that a sufficient number of elites serve as bases for exploring the space, but not so many times as to be infeasible. Meanwhile, to mitigate bias in sampling, it makes sense to sample over the course of discrete epochs. The classical *coupon collector's problem* [36] provides a suitable framework in which a company issues a large pool of coupons with n types that are distributed according to p .

Per Corollary 4.2 of [36], we have that the expected time for the event C_m of collecting m of n coupon types via IID draws from the

²⁰Evaluating f on every cell *de novo* could also be done using a state generation technique described below that is applicable to many cases of practical interest. However, this is probably inappropriate for situations we are most concerned with.

²¹We sketch the basic idea. A cell is determined by the K nearest landmarks: w.l.o.g. (i.e., up to ignorable degeneracy), we have $d(x, x_{I(1)}) < \dots < d(x, x_{I(K)})$, where I is the set of L landmark indices for the set $\{x_i\}_{i=1}^T$ of initial states. For Euclidean space, this is the same as $\|x_{I(1)}\|^2 - 2\langle x_{I(1)}, x \rangle < \dots < \|x_{I(K)}\|^2 - 2\langle x_{I(K)}, x \rangle$. A point x on the boundary of a cell can thus be produced by linear (or, according to context, integer or binary) programming. Moving towards landmarks in a controlled manner then yields a point in the interior.

distribution (p_1, \dots, p_n) satisfies

$$\mathbb{E}(C_m) = \sum_{\ell=0}^{m-1} (-1)^{m-1-\ell} \binom{n-\ell-1}{n-m} \sum_{|L|=\ell} \frac{1}{1-P_L} \quad (20)$$

with $P_L := \sum_{k \in L} p_k$. The specific case $m = n$ admits an integral representation that readily admits numerical computation,²² viz.

$$\mathbb{E}(C_n) = \int_0^\infty \left(1 - \prod_{k=1}^n [1 - \exp(-p_k t)] \right) dt. \quad (21)$$

However, the sum (20) is generally hard or impossible to evaluate in practice due to its combinatorial complexity, and it is desirable to produce useful bounds.²³

As Figures 16 and 17 illustrate, reasonably tight lower bounds turn out to be readily computable in practice,

Towards this end, assume w.l.o.g. that $p_1 \geq \dots \geq p_n$, and let $c \leq n$. (For clarity, it is helpful to imagine that $c < n$ and $p_c \gg p_{c+1}$, but we do not assume this.) To bound $\sum_{|L|=\ell} (1-P_L)^{-1}$, we first note that $\{L : |L| = \ell\}$ is the union of disjoint sets of the form $\{L : |L| = \ell \text{ and } L \cap [\lambda] = M\}$ for $M \in 2^{[\lambda]}$, where $\lambda := \min\{c, \ell\}$. Thus

$$\sum_{|L|=\ell} \frac{1}{1-P_L} = \sum_{M \in 2^{[\lambda]}} \sum_{\substack{|L|=\ell \\ L \cap [\lambda]=M}} \frac{1}{1-P_L}. \quad (22)$$

Now $P_L = P_{L \cap [\lambda]} + P_{L \setminus [\lambda]}$. If we are given bounds of the form $\pi_* \leq P_{L \setminus [\lambda]} \leq \pi^*$, we get in turn that

$$\frac{1}{1-P_{L \cap [\lambda]} - \pi_*} \leq \frac{1}{1-P_L} \leq \frac{1}{1-P_{L \cap [\lambda]} - \pi^*}.$$

If furthermore π_* and π^* depend on L only via $L \cap [\lambda]$, then

$$\begin{aligned} \frac{|\{L : |L| = \ell \text{ and } L \cap [\lambda] = M\}|}{1-P_M - \pi_*} &\leq \sum_{\substack{|L|=\ell \\ L \cap [\lambda]=M}} \frac{1}{1-P_L} \\ &\leq \frac{|\{L : |L| = \ell \text{ and } L \cap [\lambda] = M\}|}{1-P_M - \pi^*}. \end{aligned} \quad (23)$$

Meanwhile, writing $\mu := |M|$ and combinatorially interpreting the Vandermonde identity $\sum_{\mu} \binom{\lambda}{\mu} \binom{n-\lambda}{\ell-\mu} = \binom{n}{\ell}$ yields

$$|\{L : |L| = \ell \text{ and } L \cap [\lambda] = M\}| = \binom{n-\lambda}{\ell-\mu} \quad (24)$$

and in turn bounds of the form

$$\begin{aligned} \sum_{M \in 2^{[\lambda]}} \binom{n-\lambda}{\ell-\mu} \frac{1}{1-P_M - \pi_*} &\leq \sum_{|L|=\ell} \frac{1}{1-P_L} \\ &\leq \sum_{M \in 2^{[\lambda]}} \binom{n-\lambda}{\ell-\mu} \frac{1}{1-P_M - \pi^*}. \end{aligned} \quad (25)$$

Now the best possible choice for π_* is $P_{[\ell-\mu]+n-(\ell-\mu)}$; similarly, the best possible choice for π^* is $P_{[\ell-\mu]+\min\{\lambda, n-(\ell-\mu)\}}$. This immediately yields upper and lower bounds for (20), though the

²²While an integral representation of $\mathbb{E}(C_m)$ exists for generic m , it is also combinatorial in form and the result (20) of evaluating it symbolically is easier to compute.

²³A coarser approach to coupon collection than the granular approach of considering a distribution over elites would be to determine the number of samples from p required to visit every $\sigma^{(1)}$ (recall that these are the Voronoi cells of landmarks). To do this, we only need to group and add the relevant entries of p , then apply (21). However, we do not pursue this here.

alternating sign term leads to intricate expressions that are not worth writing down explicitly outside of code.

The resulting bounds are hardly worth using in some situations, and quite good in others. We augment them with the easy lower bound obtained by using the uniform distribution in (20) [5] and the easy upper bound obtained by taking $m = n$ and using (21); we also use the exact results when feasible (e.g., n small or $m = n$) as both upper and lower bounds. These basic augmentations have a significant effect in practice.

Experiments on exactly solvable (in particular, small) cases show that though the bounds for $(1 - P_L)^{-1}$ are good, the combinatorics involved basically always obliterates the overall bounds for distributions of the form $p_k \propto k^{-\gamma}$ with γ a small positive integer. However, the situation improves dramatically for distributions that decay quickly enough.

We can similarly also derive bounds along the lines above based on the deviations $\delta_k := np_k - 1$. The only significant difference in the derivation here *versus* the one detailed above is that we are forced to consider absolute values of the deviations, so although these bounds are more relevant to our context, they are also looser in practice. We provide a sketch along preceding lines. Write $\Delta_L := \sum_{k \in L} \delta_k$, so that $P_L = (|L| + \Delta_L)/n$. Assuming w.l.o.g. that $|\delta_1| \geq \dots \geq |\delta_n|$, we have $\sum_{|L|=\ell} (1 - P_L)^{-1} = \sum_{M \in 2^{[L]}} \sum_{|L|=\ell; L \cap [\lambda]=M} (1 - [\ell + \Delta_L]/n)^{-1}$. If $\pi_* \leq \Delta_L \setminus [\lambda] \leq \pi^*$ with π_* , π^* depending only on $L \cap [\lambda]$, then $\sum_{M \in 2^{[L]}} \binom{n-\lambda}{\ell-\mu} (1 - [\ell + \Delta_M + *]/n)^{-1}$ is a lower (resp., upper) bound for $\sum_{|L|=\ell} (1 - P_L)^{-1}$ for $*$ indicating π_* (resp., π^*). Meanwhile, the best possible choice for π^* is $\sum_{k=\min\{\lambda, n-(\ell-\mu)\}+1}^{\min\{\lambda, n-(\ell-\mu)\}+(\ell-\mu)} |\delta_k| \geq \Delta_L \setminus [\lambda]$ and $\pi_* = -\pi^*$.

In the near-uniform regime we also have the simple and tight lower bound $\mathbb{E}(C_m) \geq n(H_n - H_{n-m})$, where $H_n := \sum_{k=1}^n k^{-1}$ is the n th harmonic number [5, 36]. In fact this bound is quite good for the linear case in figures below and n small, to the point that replacing harmonic numbers with logarithms can easily produce larger deviations from the bound than the error itself.

D BANDWIDTH IN \mathbb{R}^N

In the setting of \mathbb{R}^N , we can deploy some analysis beforehand. First, recall the standard formula $\int_{\mathbb{R}^N} \psi(|x|) dx = \omega_{N-1} \int_0^\infty \psi(r) r^{N-1} dr$ where $\omega_{N-1} = 2\pi^{N/2}/\Gamma(N/2)$ is the Hausdorff-Lebesgue measure (i.e., generalized notion of surface area) of S^{N-1} . Writing here $\nu(x) = (2\pi)^{-N/2} \exp(-|x|^2/2)$ for the standard Gaussian, we have that $\int_{B_R(0)} \nu(x) dx = 1 - \Gamma(N/2, R^2/2)/\Gamma(N/2)$, where the numerator in the rightmost expression is the (upper) incomplete gamma function. From this it follows in particular that $\int_{B_{\sqrt{N}}(0)} \nu(x) dx \approx 1/2$.

This nominally gives us a way to relate the bandwidth (i.e., standard deviation) of a spherical Gaussian distribution to the geometry of a cell under the *Ansatz* that we are sampling near the center of a roughly spherical cell. However, in high dimensions the vast majority of a cell's volume will be near its boundary, and a spherical (or for that matter, even ellipsoidal) approximation of the cell geometry will also generally be terrible. On the other hand, a slightly more detailed analysis along the lines above yields that all but exponentially little of the probability mass of the standard Gaussian lies in

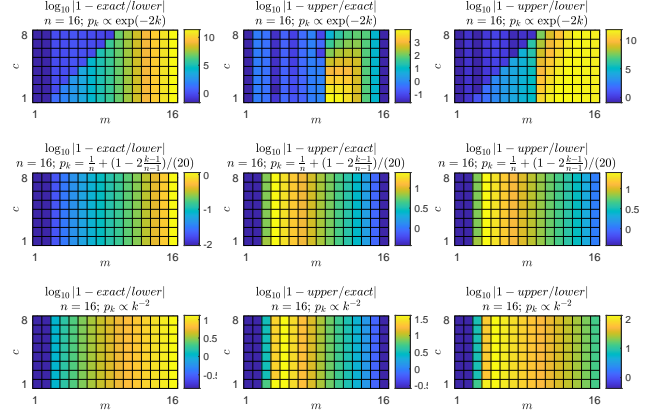


Figure 16: Comparison of exact value and (merging of various) upper/lower bounds (omitting exact calculations which are feasible for $m \lesssim 20$ from the bounds themselves) for $\mathbb{E}(C_m)$ for various probability distributions with $n = 16$. These results suggest in particular that for the case where p is approximately uniform, a readily computable lower bound is reasonably accurate.

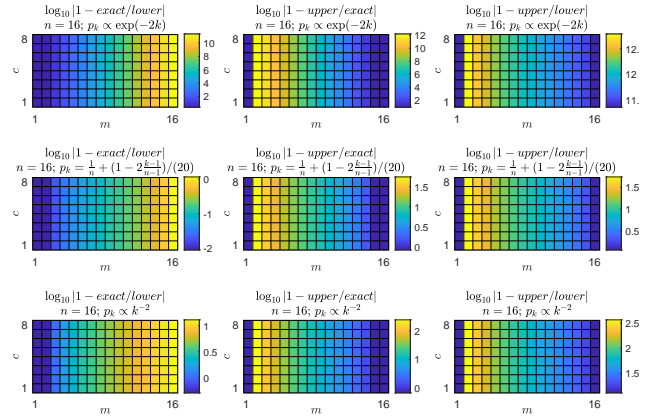


Figure 17: As in Figure 16, but without including bounds that involve a cutoff c . Again, these results suggest in particular that for the case where p is approximately uniform, a readily computable lower bound is reasonably accurate.

a thin spherical shell with radius centered at \sqrt{N} [10]. If now δ_* is the distance from the origin to the nearest part of its cell boundary and δ^* is the distance to the farthest part of its cell boundary, then we expect that $\int_{B_R(0)} \nu dx$ is nearly unity for $R < \delta_*$ and nearly zero for $R > \delta^*$, and typically with (something like) a plateau at $1/2$ for a not insignificant portion of the interval between these. In other words, we can still determine a characteristic radius of the cell by finding a bandwidth θ for Gaussian sampling that yields about half of the sample points in the cell.

E ALTERNATIVE TECHNIQUES FOR EXPLORING

For the sake of generality, first assume that we cannot estimate f (say, because X is not the sort of space that enables estimation). In this event, exploration is conceptually simple.

If parallel evaluation is not possible, simply select the point among random candidates that maximizes the differential magnitude relative to prior points in (or that by prior exploration led to) the current cell. Because the number of prior points in any cell should be fairly small (because the objective is expensive), we can usually take them *in toto*, but if this assumption is violated we can restrict consideration to at most a fixed number of points with the largest weighting components (at scale zero since we need not form a probability distribution, and possibly doing other tricks like reserving space for and uniformly sampling some additional prior points). In practice (because of approximate submodularity) we can usually settle for the approximation of a single weighting incorporating all candidate points.

If parallel evaluation is possible, we can do something similar to the landmark generation process to pick a fixed-size subset of candidates that (approximately) maximally increase the magnitude of the prior points. Alternatively, we can compute the weighting of all prior and candidate points and select the top candidates that result. (This has the benefit of being faster.)

Suppose now that we can estimate f (say by RBF interpolation): then we certainly should incorporate that estimate into the exploration process.

Again, suppose further that parallel evaluation is not possible: then we should pick the candidate point that optimizes the (W)QD-score (10) for w the weighting on cells at the prior t_+ . Alternatively, we can optimize whatever other gauge of performance we care about.

F BASELINE VERSION OF GO-EXPLORE FOR §6.1.1

G RESULTS FOR §6.2: FIGURES 18-19

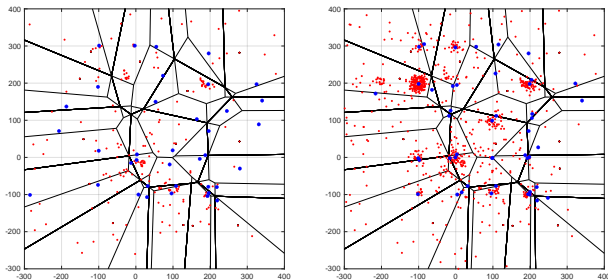


Figure 18: (L) As in the right panel of Figure 4, but for the scaled and discretized variant described in §6.2 with $\lambda = 100$. The domain is \mathbb{Z}^2 ; G is given by rounding the uniform distribution on $(\lambda \cdot [-2, 3])^2$, and g is given by rounding a spherical Gaussian away from zero. (R) As in the left panel, but for $M = 1000$.

Algorithm 5 GOEXPLOREBASELINE(f, d, L, T, K, G, M, g)

```

1: Generate landmarks as subset of initial states  $X'$  using  $G$  //
   Algorithm 2
2: Evaluate  $f$  on  $X'$ 
3: Evaluate  $\sigma^{(K)}$  on  $X'$  and initialize history  $h$  // Algorithm 3
4: while  $|h| < M$  do
5:    $E \leftarrow \bigcup_{\tau} \{\arg \min_{x \in h: \sigma^{(K)}(x) = \tau} f(x)\}$  // Elites
6:   Compute weighting  $w$  at scale  $t_+$  on  $E$ 
7:   Form diversity-maximizing PDF  $p$  // Pure exploration
8:   Compute number  $b$  of expeditions //  $b \leftarrow \lceil |E| \log |E| \rceil$ 
9:   for  $b$  steps do
10:    Sample  $x \sim p$ 
11:    Compute exploration effort  $\mu_*$  //  $\mu_* \leftarrow 10$ 
12:    //  $g(\cdot|x, \theta_0) \leftarrow$  Gaussian with covariance  $\theta_0^2 I$ 
13:    Sample  $X' \sim g^{\times \mu_*}(\cdot|x, \theta_0)$ 
14:   end for
15:   Evaluate  $f$  on  $X'$ 
16:   Evaluate  $\sigma^{(K)}$  on  $X'$  and update  $h$ 
17: end while

```

Ensure: h (obtain set E of globally diverse and locally optimal elites as above)

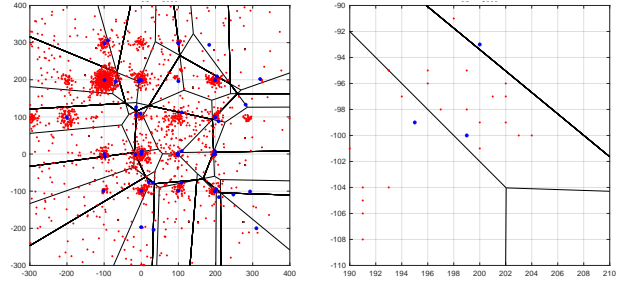


Figure 19: (L) As in the right panel of Figure 18, but for $M = 3000$. (R) Detail of the $M = 1000$ example from the left panel of Figure 18.

H ANOTHER EXAMPLE OVER \mathbb{Z}^N : REGULAR EXPRESSIONS

Figure 20 shows the minimal discrete finite automaton (DFA) for the regular expression

$$(ab(ra|cad)+(cad|ab)+ra) | (\text{bar}(car)+bad) | (\text{bar}(cab)+rad) \quad (26)$$

over the alphabet $\mathcal{A} := \{a, b, c, d, r\}$. Let Ω be the set of accepting states: both elements are circled in the figure.

Let $\iota : \{0, \dots, 5\}^{16} \rightarrow \mathcal{A}^*$ be defined by mapping (only) any initial nonzero entries to the corresponding elements of \mathcal{A} , e.g., $\iota(1, 2, 5, 1, 0, \dots, 0, 3) = abra$ and $\iota(0, 1, 2, 5, 1, 0, \dots, 0, 3) = \epsilon$, where ϵ indicates the empty string.

We define the objective

$$f(x) := \min_{\text{prefixes } w \text{ of } \iota(x)} d_{DFA}(w, \Omega) \quad (27)$$

where $d_{DFA}(w, \Omega)$ indicates the distance on the DFA digraph between the last state reached by w and the accepting states Ω . We

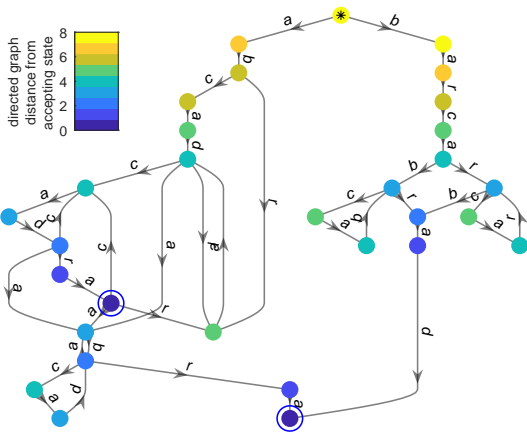


Figure 20: Minimal DFA for the regular expression (26). The initial state is shown with an asterisk; the accepting states are shown with circles. For clarity, a garbage state and transitions to it are not shown. States are colored by their digraph distance from one of the two accepting states.

take d to be Hamming distance; the global generator G to be sampling from $\mathcal{U}([5]^8 \times \{0\}^8)$; and the local generator $g(\cdot|x, \theta)$ to be uniformly changing, appending, or truncating nonzero initial entries θ times. The results of running Algorithm 1 are shown in Figures 21-24.

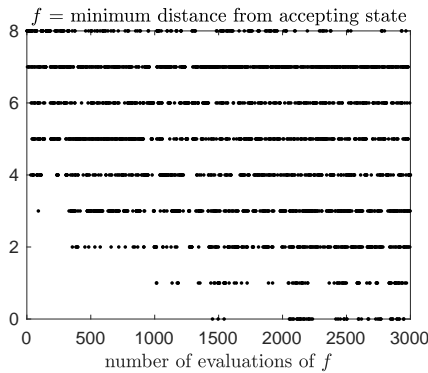


Figure 21: Values of (27) obtained from a run of Algorithm 1 with primary inputs as described in the text; $L = 15$, $T = \lceil L \log L \rceil = 41$, $K = 2$, and $\mu = 128$. Note that we reach an accepting state after fewer than 1500 function evaluations, while there are $5^8 = 390625$ strings over \mathcal{A} of length equal to the unique shortest valid string.

The problem we are solving here is easier than but related to regular language induction from membership queries alone (which is not in P: a polytime solution requires additional language queries [6]). It is morally an instance of directed greybox fuzzing [13] in which we try to obtain multiple valid strings and many long diverse prefixes of valid strings. In fact, this toy problem broadly illustrates

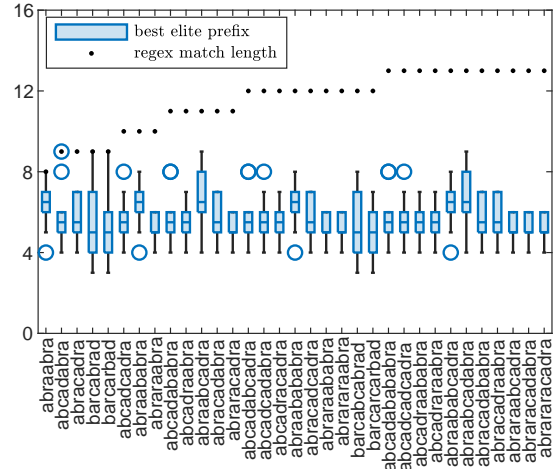


Figure 22: Boxchart detailing the extent of the best elite prefix for each short regular expression match in an ensemble of 10 runs of Algorithm 1 with primary inputs as described in the text; $L = 15$, $T = \lceil L \log L \rceil = 41$, $K = 2$, $\mu = 128$, and $M = 1000$. The boxchart shows the central quartiles as boxes, outliers (determined via interquartile range) as circles, and the range without outliers as lines. Dots indicate the length of the string indicated on the horizontal axis. Note that strings with the prefix bar are an area of relative underperformance, presumably because this area has relatively fewer extrema—and higher barriers between them—in the first place. Note also that medians are typically ≥ 5 , while $5^5 = 3125 \gg M$.

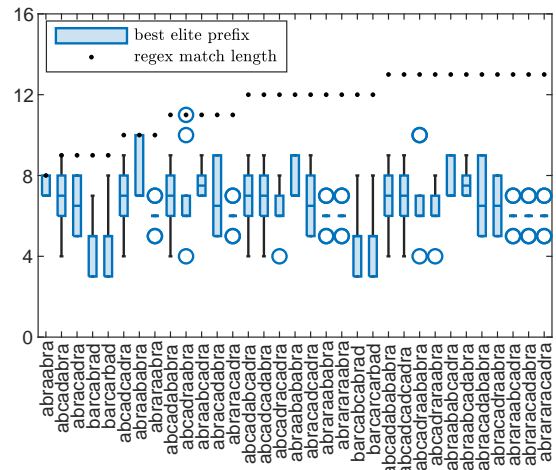


Figure 23: As in Figure 22, but for $M = 3000$.

directed greybox fuzzing in general: a control flow graph can be represented with a DFA, and in turn a regular expression [115].

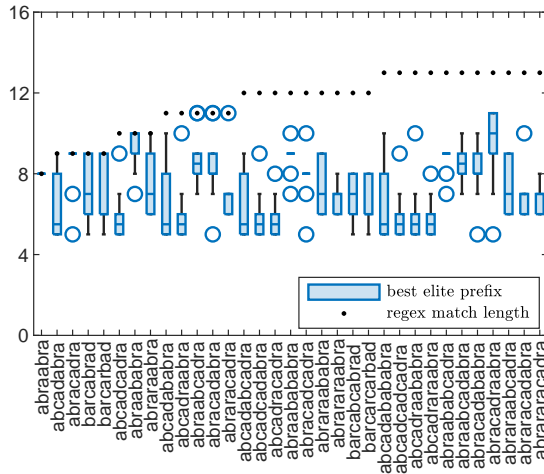


Figure 24: As in Figure 22, but for $M = 10000$. Note that one of the outliers has a prefix corresponding to the regular expression match *abracadabra*.

I OTHER EXAMPLES OVER \mathbb{F}_2^N

I.1 Supplementary figures for §6.3

Figure 25 shows the performance of Algorithm 1 on an instance of (11) with $N = 20$.

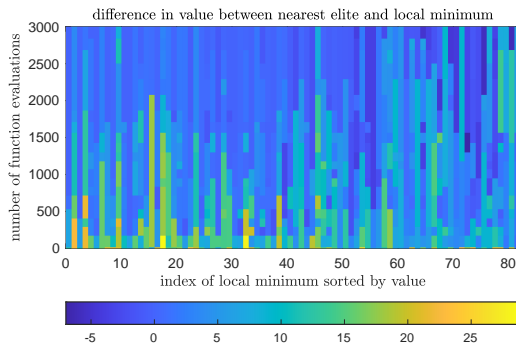


Figure 25: Another view of performance with the same data used for Figure 7. Barriers are not shown in lieu of a more detailed time evolution.

One aspect of Figure 26—the small asterisk * in the colorbar indicating a figure of merit—requires some explanation. Let $A(N, r)$ be the maximum number of points in \mathbb{F}_2^N with pairwise Hamming distance $\leq r$. The classical binary Hamming bound [85] is

$$A(N, r) \leq \frac{2^N}{\sum_{k=0}^r \binom{N}{k}}, \quad (28)$$

and its proof just amounts to observing that the denominator on the RHS is the volume of a Hamming sphere of radius r . This immediately yields a figure of merit for the Hamming distance

between elites and minima. For a set $E \subset \mathbb{F}_2^N$ of elites, let

$$r_E := \max\{r \in \mathbb{N} : |E| \leq A(N, r)\}.$$

In the extreme case that E is a “perfect” error-correcting code, then r_E is just the “distance” of the code. In general, the points of E will not be so precisely equispaced as this, and $A(N, r)$ is not easily computable, but we can nevertheless get a simple and useful figure of merit as follows. By (28),

$$r_E \leq r'_E := \max \left\{ r \in \mathbb{N} : |E| \leq \frac{2^N}{\sum_{k=0}^r \binom{N}{k}} \right\} \quad (29)$$

is easily computable. If the distance between elites and local minima tends to be significantly less than r'_E , then because Hamming balls have volume exponential in N , the elites have earned their status. In Figure 26, this is evidently the case for most of the minima, with exceptions tending to be the shallower minima.

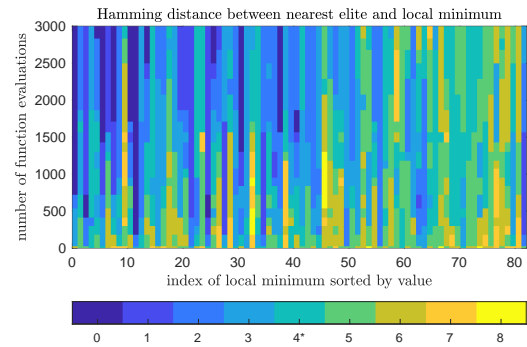


Figure 26: As in Figure 25, but for Hamming distance. The * on the colorbar indicates the figure of merit r'_E in (29).

I.2 Low-autocorrelation binary sequences

An even harder problem than that of §6.3 is that of finding low-autocorrelation binary sequences (LABS). As [32] points out, the LABS problem represents a “grand combinatorial challenge with practical applications in radar engineering and measurement.” Recall that the autocorrelation of $s \in \{\pm 1\}^N$ is $R_k(s) := \sum_{j=1}^{N-k} s_j s_{j+k}$. There are two common versions of the LABS problem, which can broadly be distinguished as being studied by physicists [35, 92] and by engineers [18]. The former, called the Bernasconi model [9], turns out to have higher barriers than the latter, suggesting a more structured landscape. It is defined via the energy function

$$f(s) = \sum_{k=1}^{N-1} R_k^2(s), \quad (30)$$

whereas the engineers’ version is defined via $f(s) = \max_{k>0} |R_k(s)|$.

Figures 27–29 show results for (30) with $N = 16$. With only 3000 evaluations, we have found 6 of 32 optimal sequences in a space with 2^{16} elements, and 15 of the 100 most optimal sequences.

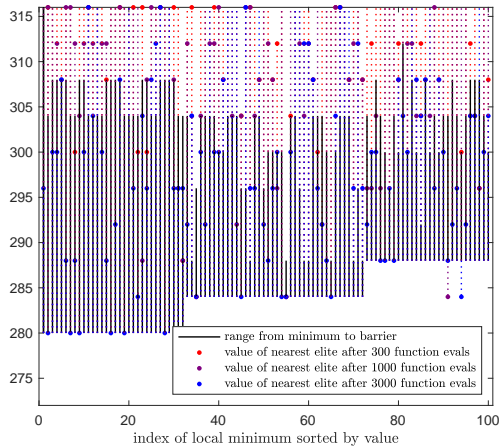


Figure 27: As in Figure 7, but for (30) with $N = 16$. Only the 100 lowest minima are shown.

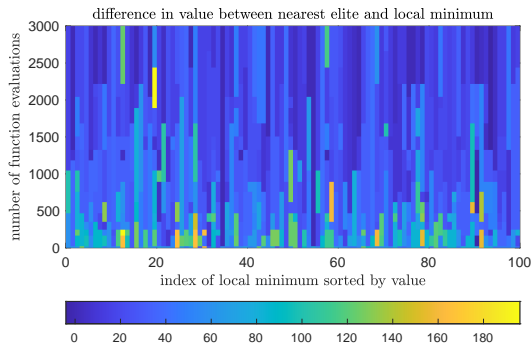


Figure 28: As in Figure 25, but for (30) with $N = 16$. Only the 100 lowest minima are shown.

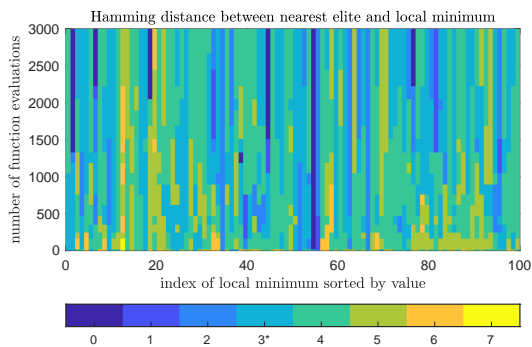


Figure 29: As in Figure 26, but for (30) with $N = 16$. Only the 100 lowest minima are shown.

1.3 Checksums and cyclic redundancy checks

Packet headers for version 4 of the Internet Protocol (IPv4) [1] include, among others, fields for the version (= 4), header length,

and a 16-bit checksum [16]. We ran our algorithm for 3000 steps on \mathbb{F}_2^{160} with

$$f = 4d_H(\text{version}, 4) + 4d_H(\text{length}, 160) + d_H(\text{nominal checksum}, \text{IPv4 checksum}),$$

$L = 6$, $T = \lceil L \log L \rceil$, $K = 2$, G uniform, and g given by bit flips with a Bernoulli parameter of q for all bits except the ones in the objective f , which have a Bernoulli parameter of $10q$, and $\mu = 128$.

This resulted in 30 elites, four of which were “perfect” in that their version, header length, and checksum were valid. Note that (although this exercise was highly artificial) this means that we obtained four distinct IPv4 headers in which 24 bits were dynamically set to precise values using just 3000 evaluations of an objective. Moreover, most elites had near neighbors in Hamming space. Below, we show the packet headers and correct checksums in hexadecimal format, with correct checksums shown in blue.

```

450555F106FE248015005326DE91FAC443C1CFD0
450555F106FE248015005326DE91FAC443C1CFD4
450755F3925640800700FB259E91F8414B80CE54
450755F3925640800700FBA59E99DA4143C0CED4
450755F3925640800700FBA59E99DB4143C0CED4
450FDCB3AAC7EB8202009BF4DE3BCAC343C1CFD0
450FDEF3AAC66B8203007D66DE3BCAC063C1CDD0
458455F106FA248015005324DE99EAC443C0CFD0
458555F106FE248015005326DE91EAC043C0CFD0
459DFA69A85A324C6B8B6866CFA398CD748D2C65
459DFA69A85A324C6B8B7066CF2398CD748D2C65
459DFA69A85A324C6B8B7866CFA398CD748D2C65
459DFAC88879365C4B8B79D4CDA318CD74896E61
459DFAC88879365C6B8BE9D4CFA338CD74892E69
459FFAC8985936586B8A4967CFB0194D748D6E68
45C3034F5DBADC3C3552E0274983B1687DC196F
45C3834F1DBA9CD3C355680F70983B1687DC196F
45C3834F5DB29CD3C3552607709A3A1687DC196F
45C3834F5DBA9CD3C3552C09709A3A16875C196F
45C3834F5DBA9CD3C3552C0F709A3B1687DE196E
45C383CB5DBA9CD3C3552C81709A3A16875C196F
45C38B5B5DBA9F92C35D13B0608A3A5F865D393B
45C38B5F5DBA9F92C35D12F0618A3A1F865D393B
45C38B5F5DBA9F92C35D1330608A3A5F865D393B
45C38B5F5DBA9F92C35D13B0608A3A5F865D393B
45C38BDF5DBA9F92C35D13B0608A3A5F865D393B
45DA7BFA1A2158A1C3AA3A7095541C1440E90080
45DA7BFA1A2158A9C3A259F09551C1440ED0080
45EA3895E95A129D3850AC069E146A8932968AEE
    
```

Similar exercises using the 32-bit cyclic redundancy check (CRC) [68] used in (e.g.) the IEEE 802.3 standard for Ethernet and many other protocols/programs suggest that more effort is required. Indeed, using the 16-bit CRC corresponding to the polynomial $x^{16} + x^{15} + x^2 + 1$ and g corresponding to uniformly flipping bits of the CRC along with 32 other bits in a notional Ethernet frame, we get only two of 19 elites with the correct CRC after 15000 evaluations of an objective that is the Hamming distance between the CRC and its nominal bits. This is in line with the general observation that

reversing CRCs is nontrivial, though readily accomplished with dedicated algorithms [113].

J EFFECT OF A BUG IN PREVIOUS VERSION OF CODE IN §K.1

After the first version of this paper was prepared, we identified and repaired a bug in the code in §K.1, then reran the examples. The original code was

```
nearInd = unique([find(inCell(:)'),nearest(1:numNearest)]);
```

For consistency with Algorithm 1, we replaced this with

```
% BUG FIXED: inBase was inCell
nearInd = unique([find(inBase(:)'),nearest(1:numNearest)]);
```

The bug meant that some of the points used to interpolate the objective were always chosen from the inhabited cell with lexicographically least $\sigma^{(K)}$ instead of the current “go-to” cell.

Fixing this bug had little quantitative effect, but suggested that the intended interpolation encourages “drilling down” into initial minima slightly more relative to initial exploration. This effect was small because the nearest points were still chosen for interpolation, and only the relatively few points in the base cell that were not sufficiently near were missed.

K SOURCE CODE

NB. The LaTeX source of a preprint version of this document contains scripts that use the code here to reproduce results/figures throughout.

K.1 goExploreDissimilarity.m

```
function [history,landmarks] = goExploreDissimilarity(f,dis,L,T,K,...
    globalGenerator,objectiveEvalBudget,isPosDef,localGenerator,...
    maxExploreEffort)

% Go-Explore instantiation serving as a quality-diversity algorithm (see
% https://quality-diversity.github.io/, and cf. multimodal optimization,
% which this can also do) using magnitude-based constructs on a
% dissimilarity space, and fundamentally using not much else besides
% mechanisms for "globally" and "locally" generating points.
%
% NB. This particular instantiation also leverages linear radial basis
% function interpolation and thus is "only" suitable for boxes in Euclidean
% space, lattices therein, and bitvectors (these last two with only
% slightly more involved exploration function handles). However, in general
% any other approach to predicting the objective f (e.g., a neural net)
% could be cleanly substituted in the code. Still more generally, a pure
% exploration mechanism based on magnitude alone could be instantiated in
% the event that objective prediction is impossible in a given situation.
%
% Inputs (with examples):
% f, function handle for objective, e.g. Rastrigin function:
% f = @(x) 10*numel(x)+x(:)'*x(:)-10*sum(cos(2*pi*x(:)));
% dis, function handle for dissimilarity (assumed symmetric), e.g.
% dis = @(x0,x1) vecnorm(x0-x1); % L2
% NB. If dis is insufficiently regular, it may be profitable to
% redefine it using the regularizeMagnitudeDimension function.
% For this reason, we don't assume dis is the L2 distance
% L, number of landmarks (<= T)
% T, number of states to generate (including landmarks, so >= L)
% K, rank cutoff <= L
% globalGenerator,
% function handle for global state generator, e.g.
% dim = 2;
% lb = -2*ones(dim,1); % lower bounds
% ub = 3*ones(dim,1); % upper bounds
% globalGenerator = ...
% @(x) diag(ub-lb)*rand(dim,1)+diag(lb)*ones(dim,1);
% objectiveEvalBudget,
% number of evaluations of f to perform
% isPosDef,
% flag to set (as per MATLAB logic, to any nonzero number) if dis
% is known a priori to be positive definite. As
% https://doi.org/10.1515/9783110550832-005 points out, this is
% the case whenever dis is (e.g.)
%
% * the usual  $\ell^p$  (or even  $\ell^p$ ) norm for  $1 \leq p \leq 2$ 
% * the usual metric on hyperbolic space
% * an ultrametric
% * the usual metric on a weighted tree
% Setting this flag allows us to avoid computing spectra that
% would otherwise be required to maintain the connection between
% weightings and diversity-saturating distributions
% localGenerator,
% function handle for exploration subroutine, e.g.
% localGenerator = @(x,theta) x+theta*randn(size(x));
% where here theta plays the role of standard deviation, and more
% generally is expected to be governed by some scalar
% "bandwidth." See note below on doing this for ints and bools,
% and also a comment in code containing the string <BANDWIDTH>
% maxExploreEffort,
% number bounding exploration effort, as measured in number of
% evaluations of f per "expedition"
%
% Outputs:
% history,
% struct with fields
% * state i.e., an input to f
% * cell the cell containing the state
% * birth the "epoch" in which the state was "born"
% * reign the last epoch in which the state was elite
% * objective the function objective value
% landmarks,
% cell (row) array of landmark states
%
% Example: the Rastrigin function
% rng('default');
% f = @(x) 10*numel(x)+x(:)'*x(:)-10*sum(cos(2*pi*x(:))); % Rastrigin
% dis = @(x0,x1) vecnorm(x0-x1);
% L = 15;
% T = ceil(L*log(L));
% K = 2;
% dim = 2;
% lb = -2*ones(dim,1); % lower bounds
% ub = 3*ones(dim,1); % upper bounds
% globalGenerator = @(x) diag(ub-lb)*rand(dim,1)+diag(lb)*ones(dim,1);
% localGenerator = @(x,theta) x+theta*randn(size(x));
% M = 3e2;
% isPosDef = 1;
% maxExploreEffort = 128;
% warning off; % to keep partialCouponCollection from complaining
% [history,landmarks] = goExploreDissimilarity(f,dis,L,T,K,...
% globalGenerator,M,isPosDef,localGenerator,maxExploreEffort);
% warning on;
% % Plot
% isCurrentElite = ([history.reign]==max([history.reign]));
% elite = {history(isCurrentElite).state};
% h_fig = figure;
% hold on;
% bar = cell2mat(landmarks);
% ind = nchoosek(1:size(bar,2),size(bar,2)-(K-1));
% for ell = 1:size(ind,1)
% h_fig = voronoi(bar(1,ind(ell,:)),bar(2,ind(ell,:)));
% for j = 1:numel(h_fig)
% set(h_fig(j),'Color',[0,0,0]);
% end
% end
% foo = cell2mat(elite);
% scatter(foo(1,:),foo(2,:),20,...
% 'MarkerEdgeColor',[0,0,1],'MarkerFaceColor',[0,0,1]);
% bar = cell2mat({history.state});
% plot(bar(1,:),bar(2,:),'r.','MarkerSize',1);
% grid on;
% daspect([1,1,1]);
% axis([lb(1)-1,ub(1)+1,lb(2)-1,ub(2)+1]);
%
% Example 2: a variant on the above with integer-valued states. Modify the
% above example along the following lines:
% scale = 100;
% f = @(x) 10*numel(x)+x(:)'*x(:)/scale^2-10*sum(cos(2*pi*x(:)/scale));
% lb = -2*ones(dim,1)*scale; % lower bounds
% ub = 3*ones(dim,1)*scale; % upper bounds
% globalGenerator = @(x) round(diag(ub-lb)*rand(dim,1)+diag(lb)*ones(dim,1));
% rafz = @(x) ceil(abs(x)).*sign(x); % round away from zero
% localGenerator = @(x,theta) x+rafz(theta*randn(size(x)));
% Zooming into the resulting figure will show the discrete nature of this
% example.
%
% NB. Elaborating on example 2, for a local generator on lattices or
% bitvectors, it is reasonable to just round/truncate the arguments of a
% Gaussian. To see why, we recall an example from section 4.1 of
% https://doi.org/10.1137/18M1164937 (preprint at
% https://arxiv.org/abs/1801.02373):
% sample = [1,0,1,-2,1,2,3,-2,1,-1]; mu = mean(sample); % 0.4
% Sigma = var(sample); % 2.7111 = (1.6465)^2
```

```

% The corresponding discrete Gaussian has the following parameters.
% Note that solving the gradient system that gives u and B requires
% evaluating (indeed, differentiating) a Riemann theta function,
% which is probably infeasible for situations of practical interest
% from our perspective.
% u = .023; B = .0587; % Taking an ample integer interval
% n = -100:100;
% Form the discrete Gaussian
% p_d = exp(2*pi*(-.5*B*n.^2+n*u));
% p_d = p_d/sum(p_d);
% Form the continuous Gaussian
% p_c = exp(-.5*(n-mu).^2/Sigma);
% p_c = p_c/sum(p_c);
% Round the argument of the continuous Gaussian
% x = linspace(min(n),max(n),10*numel(n));
% p_x = exp(-.5*(round(x)-mu).^2/Sigma);
% p_x = p_x/trapz(x,p_x);
% Rounding samples gives a pretty decent approximation to the
% discrete Gaussian here. However, in high dimensions this will be
% awful: for, as https://doi.org/10.1145/2746539.2746606 points out,
% sampling from a discrete Gaussian is hard enough that an efficient
% algorithm breaks lattice-based cryptosystems. On the other hand,
% this means that we shouldn't waste our time trying to sample from a
% discrete Gaussian in the first place, and rounding is a decent
% hack for our purposes.
figure; plot(n,p_d,'ko','n,p_c','rx',x,p_x,'b+'); xlim([-10,10]);

% Example 3: a Sherrington-Kirkpatrick spin glass, i.e., an optimization
% problem on bit vectors whose global minimum is NP-hard to compute (though
% approximable in quadratic time by https://doi.org/10.1137/20M132016X)
rng('default');
N = 20; J = triu(randn(N),1); J = (J+J')/sqrt(N);
f = @(bitColVector) (2*bitColVector(:)-1)*J*(2*bitColVector(:)-1); % SK
dis = @(x0,x1) vecnorm(x0-x1); % square root of Hamming distance
L = 10;
T = ceil(L*log(L));
K = 2;
dim = N;
lb = 0*ones(dim,1); % lower bounds: Boolean
ub = 1*ones(dim,1); % upper bounds: Boolean
globalGenerator = ... % note round!
@() round(diag(ub-lb)*rand(dim,1)+diag(lb)*ones(dim,1));
localGenerator = ...
@(x,theta) double(xor(x~=0,rand(size(x))<theta)); % bit flips
M = 3e2;
isPosDef = 1;
maxExploreEffort = 128;
warning off; % to keep partialCouponCollection from complaining
[history,landmarks] = goExploreDissimilarity(f,dis,L,T,K,...
globalGenerator,M,isPosDef,localGenerator,maxExploreEffort);
warning on;
% It is instructive to perform this example in conjunction with an analysis
% of barriers between minima of the spin glass. This particular example has
% about 1.04M states and 82 minima.
%
% NB. Most of the expensive operations in this code (function evaluations
% and dissimilarity evaluations, though not cutoff scales) could be easily
% performed in parallel with minor modifications. See in particular the
% code comments "*** CAN USE parfor HERE ***" which are not exhaustive.
%
% Last modified 20220624 by Steve Huntsman
%
% Copyright (c) 2022, Systems & Technology Research. All rights reserved.

%% Generate landmarks
[initialStates,landmarkInd,~] = generateLandmarks(globalGenerator,dis,L,T);
landmarks = initialStates(landmarkInd);

%% Assign states to cells
% Note that we are sort of overloading MATLAB terminology for cellArray:
% this is a byproduct of sticking with Go-Explore's "cell" terminology
cellArray = stateCell(dis,landmarks,K,initialStates); % a matrix
% Get unique cells to encode a set per se of inhabited cells--all
% implicitly, to save the expense of working with the cell representation.
% Use 'stable' option just so we can append efficiently later if any future
% code refactoring suggests it
[,~,cellNumber] = unique(cellArray,'rows','stable');

%% Initialize history with states used to generate landmarks
% The history (to be instantiated shortly) will detail all the states for
% which the objective is ever evaluated, their corresponding cells, the
% "epoch" in which they were "born" (i.e., the outer loop iteration during
% which the objective was evaluated on them), the last epoch in which they
% were elite (0 if never elite), and their objective values
%
% Note that we can use this information to (cheaply) reconstruct, e.g.,
% * the number K of closest landmarks used to define cells: this is
% size([history.cell],1)
% * the set of inhabited cells: up to ordering/transpose, this is
[history([history.reign]==max([history.reign])).cell]
epoch = 1;
% Objective *** CAN USE parfor HERE ***
objective = nan(size(initialStates));
for j = 1:numel(objective)
    objective(j) = f(initialStates{j});
end
% Reign
reign = zeros(size(initialStates));
for j = 1:max(cellNumber)
    inCell = find(cellNumber==j);
    [~,indArgmin] = min(objective(inCell));
    reign(inCell(indArgmin)) = epoch;
end
% The instantiation of history as a struct has the practical benefit
% that--with the possible exception of states, which might not be (column)
% vectors in general, but often will be in practice--all of the fields of
% history can be realized as matrices a la [history.cell], etc. In the
% general case, even the states can be realized as cell arrays using
% braces
initialCells = ...
    mat2cell(cellArray',size(cellArray,2),ones(1,size(cellArray,1)));
initialBirth = num2cell(epoch*ones(size(initialStates)));
initialReign = num2cell(reign);
initialObjective = num2cell(objective);
initialHistory = [initialStates;initialCells;initialBirth;...
    initialReign;initialObjective];
history = cell2struct(initialHistory,...
    ["state","cell","birth","reign","objective"],1);

%% Main loop
objectiveEvalCount = numel(history);
% Use objectiveEvalCount in lieu of numel(history) per se in order to
% better respect the evaluation budget
while objectiveEvalCount < objectiveEvalBudget

    % Identify elites (a/k/a the "archive" in Go-Explore paper--speak)
    % We keep the entire history to enhance exploration and in mind of the
    % expense of evaluating objectives for our applications
    isElite = {history.reign==epoch;
        elite = {history(isElite).state};

    % Begin a new epoch
    epoch = epoch+1;

    % <GO>

    % Compute dissimilarity matrix for elites
    dissimilarityMatrix = zeros(numel(elite));
    % Symmetry of dis is assumed (as otherwise the connection between
    % diversity saturation and weightings breaks down); hence symmetry is
    % built into dissimilarityMatrix
    for j1 = 1:numel(elite)
        for j2 = (j1+1):numel(elite)
            dissimilarityMatrix(j1,j2) = dis(elite{j1},elite{j2});
        end
    end
    dissimilarityMatrix = max(dissimilarityMatrix,dissimilarityMatrix');

    % Compute diversity-maximizing distribution on elites
    % Compute an appropriate cutoff scale to ensure a bona fide
    % diversity-maximizing distribution on elites
    if isPosDef
        % Save lots of time--avoid computing spectra over and over
        t = posCutoff(dissimilarityMatrix)*(1+sqrt(eps));
    else
        t = strongCutoff(dissimilarityMatrix)*(1+sqrt(eps));
    end
    Z = exp(-t*dissimilarityMatrix);
    % Solve for weighting while handling degeneracies
    if max(abs(Z-ones(size(Z))),[],'all') < eps^.75 % sqrt(eps) too big
        w = ones(size(Z,1),1);
    else
        w = Z/ones(size(Z,1),1);
    end
    if any(w<0)
        warning(['min(w) = ',num2str(min(w)), ' < 0: adjusting post hoc']);
        w = w-min(w);
    end
    maxDiversityPdf = w/sum(w);

    % Construct "go distribution" goPdf balancing diversity and objective
    % The improvement of the objective values should drive progress instead
    % of (e.g.) a regularization coefficient a la temperature in simulated
    % annealing: i.e., this is only implicitly dynamic
    eliteObjectiveValue = [history(isElite).objective];
    % Match top and middle quantiles of logarithm of maximum diversity PDF
    % and elite objective values en route to producing the "go
    % distribution." Note that matching ranges or moments is complicated by

```

```

% the fact that maxDivPdf has one entry that is basically zero, so its
% logarithm is hard to normalize otherwise
denom = max(log(maxDiversityPdf))-median(log(maxDiversityPdf));
denom = denom+(denom==0);
diversityTerm = (log(maxDiversityPdf)-median(log(maxDiversityPdf)))/...
    denom;
denom = max(eliteObjectiveValue)-median(eliteObjectiveValue);
denom = denom+(denom==0);
objectiveTerm = (eliteObjectiveValue-median(eliteObjectiveValue))/...
    denom;
% Encourage high diversity contributions and/or low objective values
goPdf = exp(diversityTerm(:)-objectiveTerm(:));
if numel(goPdf) == 1, goPdf = 1; end % preclude possibility of a NaN
goPdf = goPdf/sum(goPdf); % get a bona fide PDF
goCdf = cumsum(goPdf); % CDF for easy sampling

%% Determine "go effort" expeditionsThisEpoch of sampling from goPdf
% Use lower bound for collecting half of the coupons from goPdf. The
% rationale here is to systematically avoid dedicating lots of effort
% to cells that aren't promising, but to have confidence that many
% cells will still be explored
[~,lowerBound,~] = partialCouponCollection(goPdf,...
    ceil(numel(goPdf)/2),numel(goPdf));
expeditionsThisEpoch = ceil(lowerBound);
disp(['objectiveEvalCount = ',num2str(objectiveEvalCount),...
    ', expeditionsThisEpoch = ',num2str(expeditionsThisEpoch),...
    ', objectiveEvalBudget = ',num2str(objectiveEvalBudget)]);

%% </GO>

% Memorialize extrema of objective for normalization in loop below
globalMax = max([history.objective]);
globalMin = min([history.objective]);

% Inner loop over expeditions
newState = [];
for expedition = 1:expeditionsThisEpoch

    % Sample from goCdf to get a "base elite" from which to explore
    % Recall that entries of goCdf (are presumed to) correspond to
    % inhabited cells
    baseIndex = find(rand<goCdf,1,'first');

    %% <EXPLORE>

    % Determine exploration effort (from recent improvement pattern)
    % Get history of the base cell
    baseCell = stateCell(dis,landmarks,K,elite(baseIndex));
    inBase = find(ismember([history.cell]',baseCell,'rows'));
    % Determine expeditions that visit the base cell (easy), rather
    % than expeditions that start from the base cell (hard).
    %
    % Note that our method of recording history (viz., state, cell,
    % birth, reign, and objective) makes it impossible to exactly
    % reconstruct the itinerary of expeditions (i.e., which cells
    % hosted bases during a given epoch). While we could guess at
    % this--or, more sensibly, augment our records to know this--it's
    % not clear that this would actually be useful, and it would
    % increase the complexity of the code. So we avoid this
    baseEpoch = unique([history(inBase).birth]);
    % In base cell from last expedition visiting it
    oneAgo = find([history(inBase).birth]==baseEpoch(end));
    % In base cell from penultimate expedition visiting it
    if numel(oneAgo) && numel(baseEpoch)>1
        twoAgo = find([history(inBase).birth]==baseEpoch(end-1));
    else
        twoAgo = oneAgo; % could be empty in principle
    end
    % Determine normalized differential in objective over last two
    % expeditions visiting the base cell
    oneAgoObjective = [history(inBase(oneAgo)).objective];
    twoAgoObjective = [history(inBase(twoAgo)).objective];
    denom = globalMax-globalMin;
    denom = denom+(denom==0);
    bestOneAgoNormed = min((oneAgoObjective-globalMin)/denom);
    bestTwoAgoNormed = min((twoAgoObjective-globalMin)/denom);
    baseDelta = bestOneAgoNormed-bestTwoAgoNormed; % in [-1,1]
    % Determine exploration effort on the basis of prior efforts
    if epoch > 2
        priorExploreEffort = ...
            nnz([history(inBase).birth]==baseEpoch(end));
    else
        % Geometric mean of 1 and maxExploreEffort seems appropriate
        priorExploreEffort = ceil(sqrt(maxExploreEffort));
    end
    foo = max(priorExploreEffort*2^-baseDelta,1);
    exploreEffort = ceil(min(foo,maxExploreEffort));

    %% Use nearby points and those in cell to interpolate f

    % Worry later about being efficient
    %
    % Rank states in the history by dissimilarity to the base elite
    numNearest = min(numel(history),ceil(maxExploreEffort/2));
    baseDissimilarity = nan(1,numel(history));
    for j = 1:numel(history)
        baseDissimilarity(j) = dis(elite(baseIndex),history(j).state);
    end
    [~,nearest] = sort(baseDissimilarity);
    % Combine the nearest states with those in the current cell and
    % do radial basis function interpolation with a linear kernel
    % BUG FIXED: inBase was inCell
    nearInd = unique([find(inBase(:)'),'nearest(1:numNearest)']);
    x = [history(nearInd).state];
    y = [history(nearInd).objective];
    interpolant = linearRbfInterpolation(x,y);

    %% Probe, iteratively reducing bandwidth as appropriate
    numProbes = 2*maxExploreEffort;
    probe = cell(1,numProbes);
    % Initial bandwidth is big--we will bring it down to size. Note
    % that this works just fine for Booleans and Hamming distance (or
    % its ilk) along with the localGenerator function of Example 3
    % above--more generally, one can generally retool the
    % localGenerator function to play nicely with this initialization.
    % <BANDWIDTH>
    bandwidth = max(dissimilarityMatrix(baseIndex,:));
    for j = 1:numel(probe)
        % In principle we could make the localGenerator function
        % interact with available information--for example, taking the
        % in-cell and/or nearby history with objective values below
        % some quantile, getting the mean and covariance of that data,
        % and sampling from a Gaussian with those same parameters. But
        % we aren't doing that now/yet, mainly because this
        % overspecializes.
        probe(j) = localGenerator(elite(baseIndex),bandwidth);
    end
    % Compare probe cells with base cell
    probeCellArray = stateCell(dis,landmarks,K,probe); % a matrix
    probeInCell = ismember(probeCellArray,baseCell,'rows');
    % Reduce bandwidth until a significant number of probes remain in
    % the current cell (cf. Gaussian annulus theorem)
    while nnz(probeInCell) < numProbes/4
        bandwidth = bandwidth/2;
        for j = 1:numel(probe)
            probe(j) = localGenerator(elite(baseIndex),bandwidth);
        end
        probeCellArray = stateCell(dis,landmarks,K,probe); % a matrix
        probeInCell = ismember(probeCellArray,baseCell,'rows');
    end
    % Out of an abundance of caution, avoid probe collisions (this has
    % never happened in practice if problems weren't absurdly small or
    % localGenerator functions weren't poorly constructed).
    uniqueProbe = unique(cell2mat(probe)','rows');
    uniqueProbe = setdiff(uniqueProbe',...
        [history(nearInd).state'],'rows');
    probe = mat2cell(uniqueProbe,size(uniqueProbe,1),...
        ones(1,size(uniqueProbe,2)));

    %% Get biobjective data: estimated objective & weighting component
    % A local dissimilarity matrix considers all the probes at once.
    % One can easily imagine wanting to compute differential magnitudes
    % for each probe individually, but this has disadvantages. Setting
    % aside (mostly irrelevant) concerns about computational
    % complexity, the probes must eventually be treated as a batch in
    % order to perform the biobjective analysis below.
    local = [history(nearInd).state,probe];
    dissimilarityMatrix_local = zeros(numel(local));
    for j1 = 1:numel(local)
        for j2 = 1:numel(local)
            dissimilarityMatrix_local(j1,j2) = dis(local{j1},local{j2});
        end
    end
    % Compute an appropriate cutoff scale to ensure a bona fide
    % diversity-maximizing distribution on elites
    if isPosDef
        % Save time--avoid computing spectra over and over
        t_local = posCutoff(dissimilarityMatrix_local)*(1+sqrt(eps));
    else
        t_local = strongCutoff(dissimilarityMatrix_local)*(1+sqrt(eps));
    end
    % Local similarity matrix and weighting: latter is proportional to
    % diversity-maximizing distribution
    Z_local = exp(-t_local*dissimilarityMatrix_local);
    w_local = Z_local/ones(size(Z_local,1),1);
    % Estimate of objective
    f_estimate = [y,cellfun(interpolant,probe)];
    %
    biObjective = [f_estimate',-w_local'];

```

```

%% Determine quantitative Pareto dominance
% We will select the least-dominated points after normalizing both
% objectives to zero mean and unit variance a la
biObjectiveNormalized = ...
    diag(var(biObjective,0,2))\ (biObjective-mean(biObjective,2));
% we want to rank points by their Pareto domination a la
dominatedBy = nan(size(biObjectiveNormalized,2),1);
for j = 1:numel(dominatedBy)
    % This is slicker than repmat
    obj_j = biObjectiveNormalized(:,j)...
        *ones(1,size(biObjectiveNormalized,2));
    dominator = min(obj_j-biObjectiveNormalized);
    dominatedBy(j) = max(dominator);
end

%% Determine new states to evaluate after this loop
cutoff = numel(local)-numel(probe);
% 1:cutoff corresponds to stuff already in history
[~,dominanceInd] = sort(dominatedBy((cutoff+1):end));
% Taking a minimum here to prevent an out-of-bounds error was
% necessary on rare occasion (precisely once in dozens of uses
% before instituted), for reasons that aren't immediately obvious:
% no effort has yet been made to understand this
toEvaluate = ...
    probe(dominanceInd(1:min(exploreEffort,numel(dominanceInd))));
% Update in a way that lets us terminate on budget
newState = [newState,toEvaluate]; %#ok<AGROW>
objectiveEvalCount = objectiveEvalCount+numel(toEvaluate);

%% Respect the evaluation bound
if objectiveEvalCount > objectiveEvalBudget
    objectiveEvalExcess = objectiveEvalCount-objectiveEvalBudget;
    newState = newState(1:(numel(newState)-objectiveEvalExcess));
    break;
end

%% </EXPLORE>
end

%% Assign states to cells (cf. similar code @ initialization)
state = [{history.state},newState];
cellArray = stateCell(dis,landmarks,K,state); % a matrix
[~,~,cellNumber] = unique(cellArray,'rows','stable');

%% Prepare rest of history updates (cf. similar code @ initialization)
birth = [[history.birth],epoch*ones(size(newState))];
% Objective *** CAN USE parfor HERE ***
objective = nan(size(newState));
for j = 1:numel(objective)
    objective(j) = f(newState{j});
end
objective = [[history.objective],objective]; %#ok<AGROW>
% Reign
reign = [[history.reign],zeros(size(newState))];
for j = 1:max(cellNumber)
    inCell = find(cellNumber==j);
    [~,indArgmin] = min(objective(inCell));
    reign(inCell(indArgmin)) = epoch;
end

%% Update history
newState = state;
newCell = mat2cell(cellArray',...
    size(cellArray,2),ones(1,size(cellArray,1))); % a cell
newBirth = num2cell(birth);
newReign = num2cell(reign);
newObjective = num2cell(objective);
newHistory = [newState:newCell:newBirth:newReign:newObjective];
history = cell2struct(newHistory,...
    ["state","cell","birth","reign","objective"],1);
end

```

K.2 stateCell.m

```

function cellId = stateCell(dis,landmarks,K,x)

% Produce cell identifiers for states
%
% Inputs:
% dis, function handle for dissimilarity (assumed symmetric)
% landmarks,
% cell array of landmarks (versus a larger cell array of states
% and landmark indices)
% K, rank cutoff <= numel(lan) = L
% x, state(s) to map to cell
%

```

```

% Output:
% cellId,array of size [numel(x),K] whose ith row is a sorted tuple
% of the K closest landmarks (as indices, i.e., a subindex of
% landmark indices)
%
% NB. To work with states and landmarkIndex as produced by
% generateLandmarks, simply preclude executing this function by the
% assignment
% landmarks = states(landmarkIndex);
%
% Last modified 20220425 by Steve Huntsman
%
% Copyright (c) 2022, Systems & Technology Research. All rights reserved.

%% Check scalar input
% Other inputs are too tricky to check meaningfully here
if ~isscalar(K), error('K not scalar'); end
if ~isfinite(K), error('K not finite'); end
if ~isreal(K), error('K not real'); end
if K ~= round(K), error('K not integral'); end
if K < 1, error('K < 1'); end
L = numel(landmarks);
if K > L, error('K > L'); end

%%
dissimilarityFromLandmarks = nan(numel(x),L);
for i = 1:numel(x)
    for ell = 1:L
        dissimilarityFromLandmarks(i,ell) = dis(x{i},landmarks(ell));
    end
end
[~,ind] = sort(dissimilarityFromLandmarks,2);
cellId = ind(:,1:K);

```

K.3 generateLandmarks.m

```

function [initialStates,landmarkIndex,magnitude] = ...
    generateLandmarks(globalGenerator,dis,L,T)

% Generate diverse landmark states/points (we use the term state by
% reference to a dissimilarity framework for Go-Explore-type algorithms,
% which this was developed for)
%
% Inputs:
% globalGenerator,
% function handle for global state generator
% dis, function handle for dissimilarity (assumed symmetric)
% L, number of landmarks (<= T)
% T, number of points to generate (including landmarks, so >= L)
%
% Output:
% initialStates, cell array of all states produced by
% globalGenerator (for reuse)
% landmarkIndex, indices of states that are landmarks
% magnitude, magnitude of landmarks after given generations
%
% Example:
% rng('default');
% dim = 2;
% lb = zeros(1,dim);
% ub = ones(1,dim);
% globalGenerator = @() diag(ub-lb)*rand(dim,1)+diag(lb)*ones(dim,1);
% dis = @(x0,x1) vecnorm(x0-x1);
% L = 15;
% T = L^2;
% [initialStates,landmarkInd,magnitude] = ...
%     generateLandmarks(globalGenerator,dis,L,T);
% landmarks = initialStates(landmarkIndex);
% foo = cell2mat(landmarks);
% figure; plot(foo(1,:),foo(2,:),'ko')
% figure; plot(magnitude)
%
% Last modified 20220425 by Steve Huntsman
%
% Copyright (c) 2022, Systems & Technology Research. All rights reserved.

```

```

%% Check scalar inputs
% Function handles are too tricky to check meaningfully
if ~isscalar(L), error('L not scalar'); end
if ~isfinite(L), error('L not finite'); end
if ~isreal(L), error('L not real'); end
if L ~= round(L), error('L not integral'); end
if L < 1, error('L < 1'); end
if ~isscalar(T), error('T not scalar'); end
if ~isfinite(T), error('T not finite'); end
if ~isreal(T), error('T not real'); end
if T ~= round(T), error('T not integral'); end
if T < L, error('T < L'); end

```

```

%% Initial states and landmark indices
initialStates = cell(1,T);
for ell = 1:L
    initialStates{ell} = globalGenerator();
end
landmarkIndex = 1:L;

%% Initial dissimilarity matrix, scale, weighting, etc.
d0 = zeros(L);
for j = 2:L
    for k = 1:(j-1)
        % There is some superfluous indexing here for illustration
        d0(j,k) = dis(initialStates{landmarkIndex(j)},...
            initialStates{landmarkIndex(k)});
    end
end
d0 = max(d0,d0');
% The t = 0 limit is not worth considering here, as it yields either unit
% magnitude or naughty behavior. For the sake of generality (and because
% it's a one-time cost) we invoke the strong cutoff scale.
t = strongCutoff(d0)*(1+sqrt(eps));
Z0 = exp(-t*d0);
w0 = Z0\ones(size(Z0,1),1);
magnitude = nan(1,T);
magnitude(L) = sum(w0);

%% Main loop
for i = (L+1):T
    %% Propose new state to replace the one with least weighting component
    [~,ind] = min(w0);
    newState = globalGenerator();

    %% Store new state
    initialStates{i} = newState;

    %% Gauge impact on magnitude at original (strong cutoff) scale
    newRow = zeros(1,L);
    for ell = 1:L
        if ell ~= ind
            newRow(ell) = dis(newState,initialStates{landmarkIndex(ell)});
        end
    end
    d1 = d0;
    d1(ind,:) = newRow;
    d1(:,ind) = newRow';
    Z1 = exp(-t*d1);
    w1 = Z1\ones(size(Z1,1),1);

    %% Update
    if sum(w1) > magnitude(i-1)
        d0 = d1;
        w0 = w1;
        landmarkIndex(ind) = i;
        magnitude(i) = sum(w1);
    else
        magnitude(i) = magnitude(i-1);
    end
end
end

```

K.4 linearRbfInterpolation.m

```

function interpolant = linearRbfInterpolation(x,y)

% Radial basis function (RBF) interpolation using linear function (which is
% also a polyharmonic spline with exponent 1). Returns the interpolant (as
% a function handle) that fits data a la
% interpolant(x(:,j)) = y(j).
% This choice of RBF avoids the need for scaling, and in turn wrangling
% with conditioning or fancy arithmetic, and so can be implemented very
% simply. While it precludes exploiting sparsity, our intended applications
% don't presently leverage this anyway.
%
% Cf. polyharmonicRbfInterpolation.m, which generalizes this but whose
% output runs considerably slower even in the case k = 1 (NOPs take time).
%
% Example:
%     rng('default');
%     x = rand(1,10);
%     y = rand(size(x,2),1);
%     lri = linearRbfInterpolation(x,y);
%     foo = linspace(min(x),max(x),1e4);
%     bar = arrayfun(lri,foo);
%     figure;
%     plot(x,y,'ko',foo,bar,'r');
%
% 2D example:
%     rng('default');

```

```

%     x = rand(2,10);
%     y = rand(size(x,2),1);
%     lri = linearRbfInterpolation(x,y);
%     [u1,u2] = meshgrid(linspace(0,1,1e2));
%     v = nan(size(u1));
%     for j1 = 1:size(v,1)
%         for j2 = 1:size(v,2)
%             v(j1,j2) = lri([u1(j1,j2);u2(j1,j2)]);
%         end
%     end
%     figure;
%     surf(u1,u2,v);
%     shading flat;
%     hold on;
%     plot3(x(1,:),x(2,:),y,'ko');
%
% Last modified 20220429 by Steve Huntsman
%
% Copyright (c) 2022, Systems & Technology Research. All rights reserved.

%% Check x and y
if ~ismatrix(x), error('x not matrix'); end
if ~ismatrix(y), error('y not matrix'); end
if size(x,2) ~= numel(y), error('x and y sizes incompatible'); end
if any(~isreal(x(:))), error('x not real'); end
if any(~isreal(y(:))), error('y not real'); end
if any(~isfinite(x(:))), error('x not finite'); end
if any(~isfinite(y(:))), error('y not finite'); end

%% Coefficients for RBF interpolation
interpMatrix = squareform(pdist(x'));
interpCoefficient = interpMatrix\y(:);

%% Interpolant (as function handle: q = query point)
interpolant = @(q) vecnorm(x-q*ones(1,size(x,2)),2,1)*interpCoefficient;

```

K.5 posCutoff.m

```

function t = posCutoff(d)

% Minimal t such that exp(-u*d) admits a nonnegative weighting for any u >
% t. Here d is an extended real matrix with zero diagonal.
%
% Last modified 20210224 by Steve Huntsman
%
% Copyright (c) 2021, Systems & Technology Research. All rights reserved.

%% Check d matrix, square, nonnegative extended real, zero diag
if ~ismatrix(d), error('d not matrix'); end
[m,n] = size(d);
if m ~= n, error('d not square'); end
isExtendedReal = (isinf(d)|isfinite(d))&isreal(d);
if any(any(~isExtendedReal|d<0)), error('d not nonnegative extended real'); end
if any(diag(d)~=0), error('d diagonal not zero'); end

%%
t = log(n-1)/min(min(d+diag(1/n)));
lower = 0;
upper = t;
while 1-lower/upper>sqrt(eps)
    t = (lower+upper)/2;
    Z = exp(-t*d);
    w = Z\ones(size(Z,1),1);
    if all(w>0)
        upper = t;
    else
        lower = t;
    end
end

```

K.6 strongCutoff.m

```

function t = strongCutoff(d)

% Minimal t such that exp(-u*d) is positive semidefinite and admits a
% nonnegative weighting for any u > t Here d is a symmetric extended real
% matrix with zero diagonal.
%
% Last modified 20210319 by Steve Huntsman
%
% Copyright (c) 2021, Systems & Technology Research. All rights reserved.

%% Check d matrix, square, nonnegative extended real, zero diag
if ~ismatrix(d), error('d not matrix'); end
[m,n] = size(d);
if m ~= n, error('d not square'); end
isExtendedReal = (isinf(d)|isfinite(d))&isreal(d);
if any(any(~isExtendedReal|d<0)), error('d not nonnegative extended real'); end

```



```

if any(diag(d)~=0), error('d diagonal not zero'); end
if max(max(abs(d'./d-1))) > sqrt(eps), error('d not symmetric'); end

%%
t = log(n-1)/min(min(d+diag(1/n)));
lower = 0;
upper = t;
while 1-lower/upper>sqrt(eps)
    t = (lower+upper)/2;
    Z = exp(-t*d);
    spec = eig(Z);
    if min(spec)>=0
        w = Z\ones(size(Z,1),1);
        if all(w>0)
            upper = t;
        else
            lower = t;
        end
    else
        lower = t;
    end
end
end

```

K.7 partialCouponCollection.m

```
function [exact,lowerBound,upperBound] = partialCouponCollection(p,m,c)
```

```

% Calculation of the expected time for the general coupon collection
% problem in which the ith kind of coupon is drawn with probability p(i),
% and m is the number of coupon types to collect. Using p = ones(1,m)/m
% thus recovers the classical result for the uniform case. The exact result
% is computed when reasonably cheap (for details, see Corollary 4.2 of
% https://doi.org/10.1016/0166-218X(92)90177-C; for the case m = numel(p),
% see Theorem 4.1), and bounds computed more generally based on the same
% approach (both for rapidly decreasing and approximately uniform p).

```

```

% Inputs:
% p, probability distribution
% m, number of coupons to collect
% c, cutoff parameter for computations (will compute 2^c terms
% provided that c <= 16; otherwise, this will be avoided--this
% can speed things up dramatically)

```

```

% Outputs:
% exact expected time (= NaN if unknown) and lower/upper bounds

```

```

% For evaluation purposes it is useful to avoid taking exact results as
% bounds; see code cells starting with
% %% OMIT THIS FOR EVALUATION PURPOSES
% and comment them out as warranted.

```

```

% By way of (internal) documentation, see the appended LaTeX snippet.

```

```

% NB. Note that gammaln is used instead of nchoosek except when actually
% producing (vs counting) the combinations. This approach is MUCH faster.

```

```

% NB. Subsumes couponCollectionTotal.m and generalCouponCollection.m via
% special cases--these are thus deprecated.

```

```

% NB. To get just the lowerBound output argument anonymously, use something
% like this (for the second output argument):

```

```

% function nthArg = outargn(fun,n)%ok<STOUT,INUSL>
%
% % Return nth output argument from function fun. If [y_1,...,y_n,...,z]
% % = fun(inputs) then y_n = outargn(@( ) fun(inputs),n). I think this is
% % a tolerable use of eval.

```

```

% eval([' ',repmat('-',',',1,n-1),'nthArg] = fun();]);

```

```

% Last modified 20220502 by Steve Huntsman

```

```

% Copyright (c) 2022, Systems & Technology Research. All rights reserved.

```

```

%% Check p matrix, finite, real, nonnegative, sums to unity

```

```

if ~ismatrix(p), error('p not matrix'); end
isReal = isfinite(p)&isreal(p);
if ~all(isReal(:)), error('p not real'); end
if any(p<0), error('p not nonnegative'); end
if abs(sum(p)-1) > sqrt(eps)
    warning('p does not sum to unity: normalizing');
end
p = p(:)'/sum(p);

```

```

%% Check m
if ~isscalar(m), error('m not scalar'); end
if ~isfinite(m), error('m not finite'); end
if ~isreal(m), error('m not real'); end

```

```

if m ~= round(m)
    error('m not integral');
end
if m < 1, error('m < 1'); end

```

```

%% Check c
if ~isscalar(c), error('c not scalar'); end
if ~isfinite(c), error('c not finite'); end
if ~isreal(c), error('c not real'); end
if c ~= round(c)
    error('c not integral');
end

```

```

if c < 1, error('c < 1'); end
if c > 16
    avoid_c = 1;
    warning('c too big to quickly compute corresponding bounds: avoiding');
else
    avoid_c = 0;
end

```

```

%% Check number of coupon types is achievable (note restriction to support)
if m > nnz(p), error('numCouponTypes > nnz(p)'); end

```

```

%% Annoying corner case

```

```

if m == 1
    warning('m = 1');
    exact = 1;
    lowerBound = 1;
    upperBound = 1;
    return;
end

```

```

p = sort(p,'descend');
n = numel(p);
exact = NaN;

```

```

%% [EXACT] Produce exact result for both bounds if easy, else m = n bound

```

```

if n <= 16
    exact = 0;
    for ell = 0:(m-1)
        ind = nchoosek(1:n,ell);
        pInd = reshape(p(ind),size(ind));
        sign = (-1)^(m-1-ell);
        S = sum(1./(1-sum(pInd,2)));
        exact = exact+sign*nchoosek(n-ell-1,n-m)*S;
    end
    %% OMIT THIS FOR EVALUATION PURPOSES
    lowerBound = exact;
    upperBound = exact;
    return;
end

```

```

%% [TOTAL] Get "total" result for m = n, which is also an upper bound
% Theorem 4.1 of https://doi.org/10.1016/0166-218X(92)90177-C yields
% expectation for total coupon collection as an integral that admits
% straightforward numerical computation
% disp('Computing for case m = n');
f = @(t) 1-prod(1-exp(-p(:)*t),1);
x = 1; while f(x) > eps, x = 10*x; end % OK upper limit for integral
t = linspace(0,x,1e4);
total = trapz(t,f(t));

```

```

%% Initialize bounds
lowerBound = 0;
upperBound = total;

```

```

%% Return total result if m = n

```

```

if m == n
    exact = total;
    %% OMIT THIS FOR EVALUATION PURPOSES
    lowerBound = exact;
    upperBound = exact;
    return;
end

```

```

%% Now we'll have to compute less trivial bounds (c permitting)...

```

```

% See notes
if ~avoid_c
    %% Form power set of 1:c
    % disp('Generating power set of 1:c');
    powerSet = false(2^c,c);
    for j = 1:c
        powerSet(:,j) = bitget((0:(2^c-1))',j);
    end
    %% Bounds assuming rapid decay of p
    % Based on exact result of Corollary 4.2 in
    % https://doi.org/10.1016/0166-218X(92)90177-C
    % disp('Computing bounds for rapidly decaying p');

```


K.8 goExplorePerfEval.m

```

function [qd,wqd,numEvals,mag,misc] = ...
    goExplorePerfEval(history,dis,varargin)

% Optional third, fourth argument of minObjective and maxObjective to
% facilitate benchmarking
%
%     figure; plot(numEvals,wqd,'b.-',numEvals,qd,'r.-')
%
% Last modified 20220630 by Steve Huntsman
%
% Copyright (c) 2022, Systems & Technology Research. All rights reserved.

numEpochs = max([history.birth]);
% Only nominal error checking for minObjective, maxObjective arguments
narginchk(2,4) % optional argument for minObjective, maxObjective
if nargin == 4
    minObjective = varargin{1};
    maxObjective = varargin{2};
elseif nargin == 3
    minObjective = varargin{1};
    maxObjective = max([history.objective]);
else
    minObjective = min([history.objective]);
    maxObjective = max([history.objective]);
end
qd = nan(1,numEpochs);
wqd = nan(1,numEpochs);
numEvals = nan(1,numEpochs);
mag = nan(1,numEpochs);

%%
misc = [];

for j = numEpochs:-1:1 % go backwards to get proper scale
    eliteInd = find(([history.reign]>j)&([history.birth]<=j));
    elite = {history(eliteInd).state};
    objective = [history(eliteInd).objective];

    %% Dissimilarity matrix for elites
    dissimilarityMatrix = zeros(numel(elite));
    % Symmetry of dis is assumed (as otherwise the connection between
    % diversity saturation and weightings breaks down); hence symmetry is
    % built into dissimilarityMatrix
    for j1 = 1:numel(elite)
        for j2 = (j1+1):numel(elite)
            dissimilarityMatrix(j1,j2) = dis(elite{j1},elite{j2});
        end
    end
    dissimilarityMatrix = max(dissimilarityMatrix,dissimilarityMatrix');

    %% Diversity-maximizing distribution on elites AT COMMON SCALE
    if j == numEpochs
        t = posCutoff(dissimilarityMatrix)*(1+sqrt(eps));
    end
    Z = exp(-t*dissimilarityMatrix);
    w = Z/ones(size(Z,1),1);
    if any(w<0)
        warning(['min(w) = ',num2str(min(w)),' < 0: adjusting post hoc']);
        w = w-min(w);
    end

    %% Cell counts etc
    cellCount = nan(size(w));
    cellMax = nan(size(w));
    cellMin = nan(size(w));
    for k = 1:numel(elite)
        baseCell = history(eliteInd(k)).cell';
        inBase = find(ismember([history.cell]',baseCell,'rows'));
        cellCount(k) = numel(inBase);
        cellMax(k) = max([history(inBase).objective]);
        cellMin(k) = min([history(inBase).objective]);
    end

    %% Performance metrics per epoch
    qd(j) = sum(maxObjective-objective)/(maxObjective-minObjective);
    wqd(j) = (maxObjective-objective)*(w*numel(w)/sum(w))/(maxObjective-minObjective);
    numEvals(j) = nnz([history.birth]<=j);
    mag(j) = sum(w); % magnitude
    % Miscellany
    misc(j).objective = objective;
    misc(j).w = w;
    misc(j).cellCount = cellCount;
    misc(j).t = t;
end

```